Enniatin B induced inflammatory response and cell death in RAW 267.4 murine macrophages

Anders Ødegaard Gammelsrud

Master thesis in toxicology
Faculty of Mathematics and Natural Sciences
Department of Biology

UNIVERSITY OF OSLO

2011

Enniatin B induced inflammatory response and cell death in RAW 267.4 murine macrophages

2011

Enniatin B induced inflammatory response and cell death in RAW 267.4 murine macrophages.

Anders Ødegaard Gammelsrud

http://www.duo.uio.no/

Trykk: Reprosentralen, Universitetet i Oslo

Forord

Oppgaven er hovedsakelig presentert som et artikkelmanuskript, men relevant bakgrunnsinformasjon er beskrevet i "*Background*".

Arbeidet i denne masteroppgaven er gjennomført ved Veterinærinstituttet (VI), seksjon for kjemi og toksikologi og ved avdelingen for luftforurensning og støy (MILS), divisjon for miljømedisin ved Folkehelseinstituttet (FHI). Arbeidet ble påbegynt høsten 2009 og ble ferdigstilt våren 2011. Jeg har vært så heldig å ha Jørn A. Holme som veileder og Anita Solhaug som medveileder. Intern veileder har vært Professor Steinar Øvrebø ved det biologiske institutt, Universitet i Oslo.

Jeg vil begynne med å takke seksjonsleder ved VI, Jens Børsum, og administrativt ansvarlig for oppgaven, Gunnar Sundstøl Eriksen, for at jeg fikk anledningen til å jobbe med akkurat denne oppgaven.

Spesielt stor takk til Jørn og Anita for fantastisk bra veiledning. Dere har begge vært motiverende og engasjerende å jobbe med, og er veldig flinke til å lære bort! Jeg har lært utrolig mye gjennom denne perioden.

Jeg vil også takke Lada Ivanova for god opplæring og hjelp i starten på oppgaven.

Også takk til alle på MILS, hvor jeg har tilbrakt mye tid på Western-lab og ELISA-lab. Ekstra takk til Hans Jørgen Dahlmann som har gitt opplæring i flow cytometry og Rune Becher for introduksjon i immunocytokjemi.

Takk til venner og familie, og ekstra takk til kjæresten min.

Oslo, Mai 2011.

Anders Ø. Gammelsrud

Sammendrag

Dette studiet er gjort for å undersøke cytotoksiske og inflammatoriske effekter av mykotoksinet, enniatin B (EnnB) på makrofager av museopphav (RAW 264.7 celler). EnnB produseres av forskjellige stammer av muggsoppen *Fusarium* og finnes som en hyppig forekommende kontaminant i kornblandinger som benyttes til mat for mennesker og dyr. For dette studiet er EnnB produsert fra *F. avenaceum*-kulturer benyttet. De cytotoksiske egenskapene til EnnB skyldes mest trolig evnen til å danne porer for transport av kationer i biologiske lipidmembraner. Undersøkelser er gjort i forhold til karakterisering av celledød, påvirkning av celleproliferasjon og produksjon av cytokiner (betennelsesmarkører) utløst av ulike nivåer mykotoksin.

Resultatene viser at EnnB eksponering fører til en opphopning eller arrest av celler i G1-fasen av cellesyklus, dette ble undersøkt ved bruk av flow cytometri og ved analyse av cellesyklusrelaterte proteiner ved Western blotting. Bruk av fluorescence mikroskop viste at celler eksponert for EnnB får morfologiske trekk assosiert med apoptose, i tillegg ble skader på lysosomene observert ved bruk av elektron mikroskop. Videre vises en oppregulering av aktivert caspase-1 og i celler preinkubert med lipopolysakkarid (LPS) etterfulg av EnnB eksponering ble det målt høye verdier av interleukin-1 beta (IL-1β) ved bruk av ELISA. Ved å benytte en caspase-1 spesifikk hemmer ble denne utskillelsen av cytokiner redusert. På bakgrunn av disse resultatene antar vi at EnnB fører til en aktivering av et proteinkompleks, inflammasomet, etterfulgt av caspase-1 aktivering og utskillelse av IL-1β.

Table of contents

Aims of study

The aim of this study was to characterize the effects of Enniatin B on the murine macrophage cells line, RAW 264.7. In order to better understand the mechanism of cytotoxicity several different assays have been used to investigate:

- Cell death and cell proliferation
- DNA damage response (DDR)
- Cell cycle regulation
- Production of cytokines

This master thesis is a part of a project funded by the Norwegian Research Council, *Toxicological characterization of selected secondary fungal metabolites in Norwegian grain* (grant number 185622), which is managed by Gunnar Sundstøl Eriksen. The project was started in 2008 and some preliminary work had been done before I started working with the thesis. This work include the TUNEL assay (**fig. 4D and 4E**) and the alkaline comet assay (**fig. 8A and 8B**), both done by Dr. Anita Solhaug. In addition, the GM1 Immunofluorescence assay (**fig. 9A and 9B**), and electron microsocopy pictures (**fig. 10A and 10B**) done by Béatrice Dendelé, Dr. Dominique Lagadic-Gossmann, Inserm U620, Université Rennes and Dr. Anita Solhaug.

Abbreviations

ATM, Ataxia telangiectasia mutated;

ATR, Ataxia telangiectasia and Rad3-related protein;

CDK, Cyclin dependent kinase;

CDKI, Cyclin dependent kinase inhibitor;

Chk, Checkpoint kinase;

DAMP, Danger associated molecular patterns;

EnnB, Enniatin B;

IL-1β, Interleukin-1 beta;

LPS, Lipopolysaccharide;

PAMP, Pathogen associated molecular pattern;

PRR, Pattern recognition receptor;

Background

1.1 Mycotoxins

Mycotoxins are secondary metabolites produced under appropriate environmental conditions by filamentous fungi, mainly *Aspergillus spp*., *Penicillum spp*., and *Fusarium spp*. Mycotoxins are common contaminants of grains like wheat, barley, maize, and rice, and they can evoke a broad range of toxic effects, including carcinogenicity, neurotoxicity, as well as reproductive and developmental toxicity. Mycotoxins are also found in the soil and indoor environments, especially water-damaged buildings provide excellent growth conditions for several mold species [1,2]. For these reasons, mycotoxins pose a health risk to both humans and animals. The total number of potential toxic metabolites of fungi has been estimated to be in the thousands [6].

Annual economical losses are caused by mycotoxins all over the world, in the grain trade and to the marketing of foods and feeds. In the US losses in wheat and barley attributable to the *Fusarium*-mycotoxins have been estimated to about 2900 million dollars each year [7]. In addition, there are financial losses due to decreased productivity of farm animals [8].

The most common mycotoxin producing fungi in the northern temperate regions are *Fusarium spp*. The genus *Fusarium* includes several species, which are pathogens of maize and small grains, causing stem and ear rot with severe crop yield reduction. In addition to their patogenicity, some *Fusarium* strains are also capable of producing mycotoxins, which can accumulate either preharvest or in stored grains [9]. Mycotoxins produced by *Fusarium spp*., include trichothecenes and zearalenone, and the emerging mycotoxins fusaproliferin, beauvericin, enniatins, and moniliformin. In the Nordic countries the most prevalent *Fusarium* species, F. avenaceum, is known to produce emerging mycotoxins like beauvericin, enniatins, and moniliformin [10].

1.2 Cell death

In order to accurately classify different forms of cell death, various characteristics may be used; morphological appearance (which may be apoptotic, necrotic, autophagic, or associated with mitosis); enzymatic criteria (with and without involvement of nucleases or distinct classes of proteases, such as caspases, calpains, cathepsins, and transglutaminases); functional aspects (programmed or accidental, physiological or pathological); or immunological characteristics (immunogenic or non-immunogenic) [11]. Based on criteria formulated by the Nomenclature Committee on Cell Death (NCCD) any of the following features should be observed in cells classified as dead: (I) the loss of plasma membrane (PM) integrity, defined by uptake of vital dyes (.i.e. PI) *in vitro*; (II) complete cellular fragmentation into apoptotic bodies; or (III) *in vivo*, engulfment by an adjacent cells [12]. Described below is apoptotic, necrotic, and autophagic cell death, which are morphological distinctive forms of cell death

Apoptosis. Apoptosis is a form of cell death was first termed by Kerr *et al*. [13], apoptosis and programmed cell death (PCD) is not synonymous because PCD occurring in the physiological development can have non-apoptotic features [14]. It has been estimated that ~100 000 cells are produced every second through mitosis, and about the same number die every second by apoptosis in a human being [15]. Apoptosis is therefore essential in maintaining homeostasis in multicellular organisms. During development, apoptosis is an active form of cell death which is genetically timed [16].

Apoptosis is accompanied by rounding-up of the cell, retraction of pseudopodes, reduction of cellular volume (pyknosis), chromatin condensation, nuclear fragmentation (karyorrhexis), little or no ultrastructural modifications of cytoplasmic organelles, blebbing of the PM (PM integrity maintained until the final stages of the apoptotic process), and engulfment by nearby phagocytes (*in vivo*) [12].

Both external stimuli, such as cell death ligands released during inflammation, and intrinsic stimuli, caused by alteration of cellular function and metabolism can trigger apoptosis. Generally, the cellular membrane of apoptotic cells remains intact and the process causes less inflammation than, i.e. necrosis [17].

Apoptosis is executed by involvement of several enzymes activated through signalling pathways. Proteolytic activation of caspases (cystein aspartyl-specific proteases) is a typical biochemical feature of apoptosis [18]. Caspases are a family of proteases and are synthesized as proenzymes, which are activated by proteolytic cleavage or by interactions with an allosteric activator. The caspases involved in execution of apoptosis may be divided into initiator caspases (caspase-2, -8, -9, -10) and effector caspases (caspase-3, -6, -7) [19].

Caspase activation can be carried out by either the extrinsic (death-receptor mediated) or the intrinsic (mitochondria mediated) pathway [16]. The extrinsic pathway is triggered by binding of cell surface receptors and the ligands, such as tumor necrosis factor (TNF) or Fas ligand (FasL). The death receptors mediate apoptotic signals through death domains and death effectors domain modular protein motifs. Activated death receptor induces formation of the death-inducing signalling complex (DISC), which activates multiple procaspase-8 molecules through the adaptor molecule Fas-associated death domain protein [20]. Further, activated caspase-3 triggers enzymes responsible for apoptosis, which result in phosphatidylserine externalization, nuclear condensation, and DNA fragmentation [21].

The intrinsic apoptotic pathway is triggered in response to intracellular stress, such as cytokine deprivation, ionizing radiation, and chemotherapeutics [21]. This pathway is characterized by permeabilization of the outer mitochondrial membrane, and is regulated by the B cell lymphoma (Bcl)-2 family of proteins [20]. The permeabilization of the outer mitochondrial membrane leads to apoptosis either through release of mitochondrial molecules, such as cytochrome c, or as a result of lost mitochondrial function [22]. Cytosolic cytochrome complexes with apoptosis protein factor-1 (APAF-1) and caspase-9, in a complex called the apoptosome, resulting in activation of caspase-9 and caspase-3 [20]. The mitochondria are also involved in caspase independent cell death, in which apoptose-inducing factor (AIF) and endonuclease G are major players [23].

Recently, another form of cell death, pyroptosis, has been characterized. This novel form of cell death is induced by infection with *Salmonella* and *Shigella* species [24]. Pyroptotic cell death is caspase-1 dependent and involved in activation of a multiprotein complex called the inflammasome, which results in release of inflammatory cytokines [25]. Macrohages undergoing pyroptosis are described to exhibit some features typical of apoptosis and some traits associated with nerotic cell death [26].

Necrosis. A necrotic cell death is morphologically characterized by gain in cell volume (oncosis), swelling of organelles, plasma membrane rupture followed by loss of intracellular contents. Necrosis is by Kroemer and Martin [21] regarded as an accidental cell death, and occurs when cells are exposed to high concentrations of detergents, oxidants, ionophores, or severe pathological insults [17]. Processes implicated to be involved in necrotic cell death are mitochondrial alterations (uncoupling, production of reactive oxygen species (ROS), and mitochondrial membrane permeabilization), lysosomal changes (ROS production, lysosomal membrane permeabilization), nuclear changes, lipid degradation, and increase in the cytosilic Ca^{2+} concentration resulting in mitochondrial overload and activation of non-caspase proteases (calpains and cathepsins) [12]. In absence of common biochemical features, necrotic cell death is mostly identified in negative terms by absence of apoptotic or autophagic markers [12].

Autophagy and autophagic cell death. There is a difference between the process of autophagy and an autophagic cell death. Autophagy is essential for the removal of damaged organelles and long-lived cytosolic macromolecules to maintain energy homeostasis, and hence cell survival, during starving conditions. However, when excessive, autophagy results in autophagic cell death [27].

An autophagic cell death is morphologically defined (by transmission electron microscopy) as a type of cell death that occurs in the absence of chromatin condensation, and is accompanied by massive autophagic vacuolization of the cytoplasm [28]. Cytoplasmic material is sequestered within autophagosomes for degradation by the lysosomes, and the following fusion between autophagosomes and lysosomes.

Autophagy can be triggered in infected host cells, presumably as a host defence mechanism for eliminating the pathogen without disposing of the entire cell [29].

Different pathways of cell death are shown in **Figure 1**.

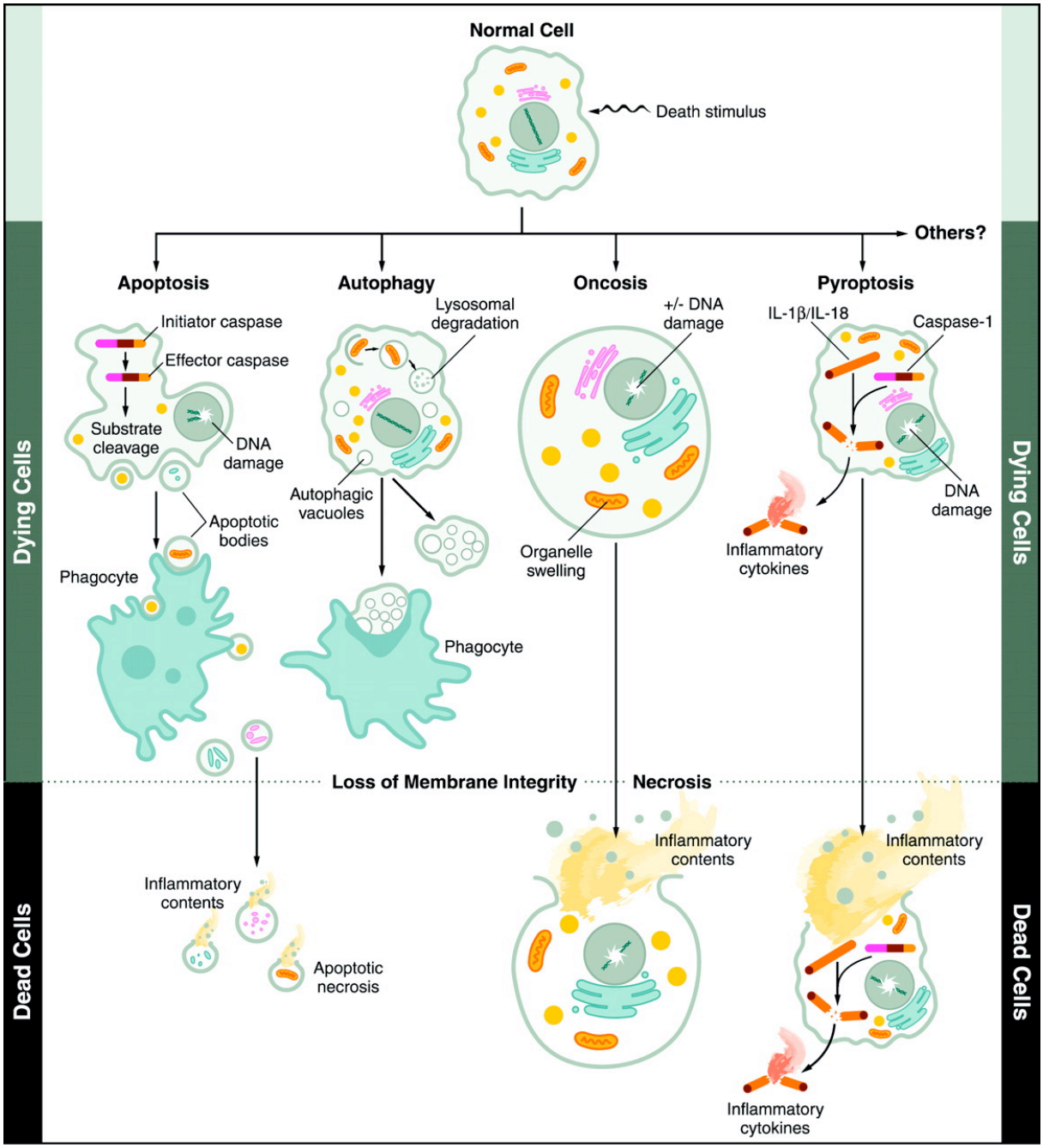

Figure 1. Pathways leading to cell death. Shown are the different forms of cell death initiated by death stimuli, apoptosis, autophagy, and necrosis. The caspase-1 dependent pyroptotic cell death is also shown. As the figure indicates, other undescribed pathways may also exist [4].

1.3 DNA-damage response (DDR)

DNA damage may arise from errors during the process of DNA replication, as well as through genotoxic stress from reactive cellular metabolites and exogenous stimuli, i.e. ionising radiation, ultraviolet light, or cigarette smoke [30]. In response to DNA damage cells will respond by activating DNA repair and DNA damage signalling pathways [31]. Different types of DNA damage trigger different damage responses through activation of specific protein kinases [32]. The kinase ATM (ataxia-telangiectasia mutated) is a major sensor of double-strand (ds) DNA breaks and larger chromatin alterations. ATR (ATM and Rad3-related) is the main sensor of single-strand (ss) DNA breaks and is activated most strongly by stalled replication forks [33]. ATM and ATR initiate cell cycle arrest by activating specific checkpoint kinases (Chk), Chk2 and Chk1, respectively, allowing time for DNA repair. ATM and ATR may also phosphorylate the tumor suppressor p53 directly or indirectly through Chk1/2. Phosphorylation of p53 by Chk1/Chk2 is followed by p53 translocation from cytosol to the nucleus. Nuclear p53 promotes the transcription of cell cycle arresting genes, allowing for DNA repair, and or transcription of pro-apototic genes [19]. The tumor suppressor protein p21 (Waf1/Cip)1 (p21) is one such protein, and it acts as an inhibitor of cell cycle progression. This protein is associated with G_1-arrest in the cell cycle [34], and phosphorylated p53 upregulates p21 transcription via a p53 responsive element [35].

1.4 Cell cycle and cell cycle regulation

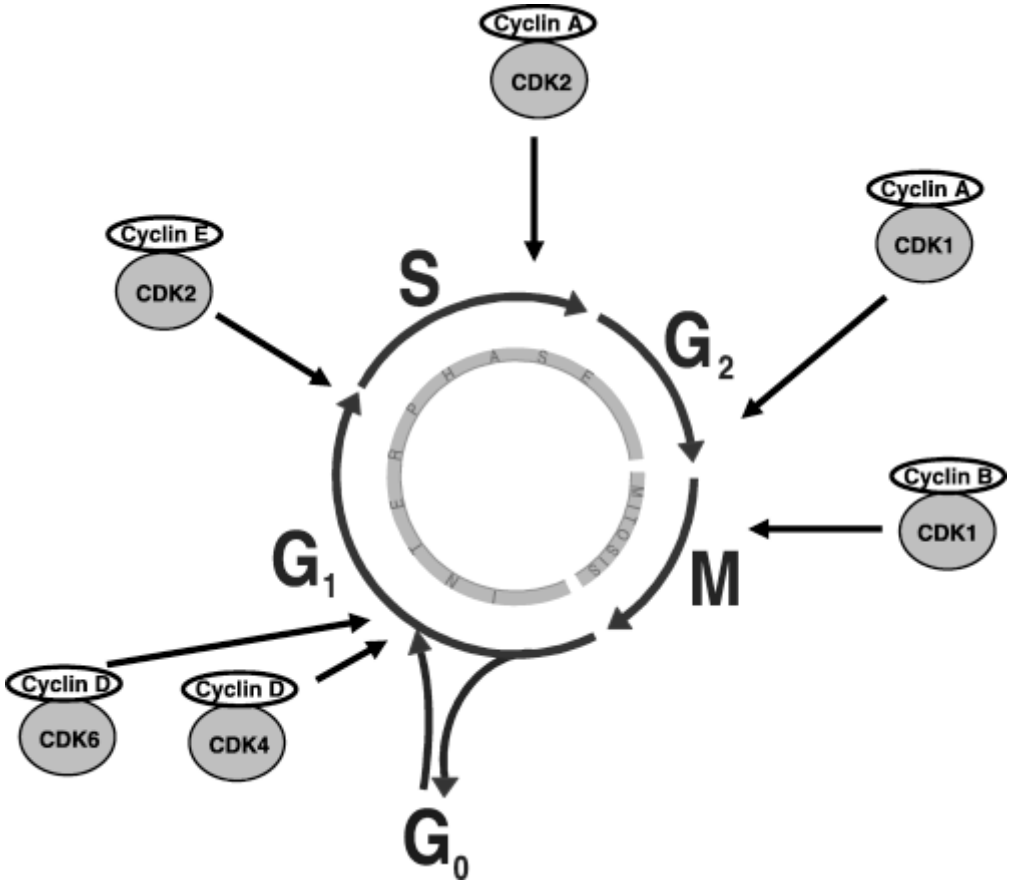

Figure 2. The stages of the cell cycle. Shown are the activity sites of cyclins and cyclin dependent kinases (CKDs) [3].

Cell division consists of two consecutive processes, the replication of DNA and segregation of replicated chromosomes into two separate cells. Originally, cell division was divided into two stages: the mitosis (M), which is the process of nuclear division and the interphase, the interlude between two M phases (**Figure 2**). The mitosis includes the stages prophase, metaphase, anaphase and telophase, where the interphase includes the G_1, S, and G_2 phases [36] [3]. The G_1 phase, where the cell is preparing for DNA synthesis is followed by the S phase in which the actual DNA replication occurs. In the G_2 phase the cell is preparing for mitosis. Cells can in G_1, before commitment to DNA replication, enter a resting state called G_0. In humans, cells in G_0 accounts for the major part of the non-growing and non-proliferating cells [3].

The progression of cells through the cell cycle is regulated by different cyclin and cyclin-dependent kinase (CDK) complexes. Nine different CDKs have been identified, with five of these active during the cell cycle; G_1 (CDK4 and CDK6), S (CDK2), G_2 and M (CDK1) [3]. The levels

of CDK proteins remain stable during the cell cycle, while the levels of most cyclins rise and fall as they are periodically activated [37]. The D-type cyclins (D1, D2, and D3) bind to CDK4 and CDK6 and are essential for entry in G_1. In contrast to the other cyclins, the D-type is not expressed periodically, but is synthesized as long as growth factor stimulation persists [38]. Cyclin E, another G_1 cyclin, associates with CDK2 to regulate progression from G_1 into the S phase [39], while binding of cyclin A with CDK2 is required for S phase progression [40]. In late G_2 and early M, cyclin A complex with CDK1 to promote entry into M. The mitosis (M) is then further regulated by cyclin B in complex with CDK1 [41].

The activity of CDKs can be counteracted by cell cycle inhibitory proteins, called CDK inhibitors (CDKI). The CDKIs bind to CDKs alone or to the CDK-cyclin complex and regulate CDK activity. Two distinct families of CDKIs have been identified, namely the INK4 family and the Cip/Kip family [42]. The INK4 family consists of p15 (INK4b), p16 (INK4a), p18 (INK4c), p19 (INK4d), which inactivate CDK4 and CDK6 of G_1. The second family of inhibitors, the Cip/Kip family, includes p21 (Waf1/Cip1), p27 (Kip1), and p57 (Kip2), which inhbit CDK2 of G_1, and to a lesser extent, CDK1-cyclin B complexes [43]. In addition, p21 also inhibits DNA synthesis by binding to and inhibiting the proliferating cell nuclear antigen (PCNA) [44].

1.5 Inflammatory response and the NLRP3 inflammasome

In correlation with Matzingers's "danger hypothesis", proposed for adaptive immune responses [45], emerging literature suggest that innate immunity serves as a system for sensing signals of "danger", such as pathogenic microbes or host-derived signals of cellular stress, while remaining unresponsive to non-dangerous motifs, such as normal host molecules, dietary antigens, or commensal gut flora [5]. Innate immunity has a wide range of germline-encoded pattern recognition receptors (PRRs) in order to detect invariant microbial motifs. PRRs are expressed by cells at the front line of defence against infection, consisting of macrophages, monocytes, dendritic cells, neutrophils, and epithelial cells, as well as cells of the adaptive immune system. The PRRs include the transmembrane associated Toll-like receptors (TLRs) [46], the C-type lectin receptors (CLRs) [47], the RIG-like helicases (RLHs) [48], cytosolic DNA sensors (DAI and AIM2) [49,50], and members of the NOD-like receptor (NLR) family [51]. The individual PRRs recognize products and elements of all the major microbial pathogens; bacteria, viruses, yeast, and parasites. In addition, the PRRs are able to sense endogenous products, or danger associated molecular patterns (DAMPs) that are released from damaged or dying cells [52]. Examples of DAMPs are nucleic acids, ATP, and uric acid crystals, which trigger many of the same responses that are induced upon detection of microbes during innate immunity [52]. However, these responses are detrimental to the host, often contributing to inflammation.

The NLRs, which are cytosolic sensors, are characterized by the presence of a nucleotide-binding oligomerization (NACHT) domain, which is commonly flanked by C-terminal leucine-rich repeats (LRRs) and a N-terminal caspase recruitment domain (CARD or a pyrin domain (PYD).The NLRP3 inflammasome, which is the currently most characterized inflammasome, consists of the NLRP3 scaffold, the apoptotic speck protein containing a C-terminal caspase recruitment domain (ASC), and caspase-1. Other inflammasomes are made up of similar constituents (**Figure 3**) [5].

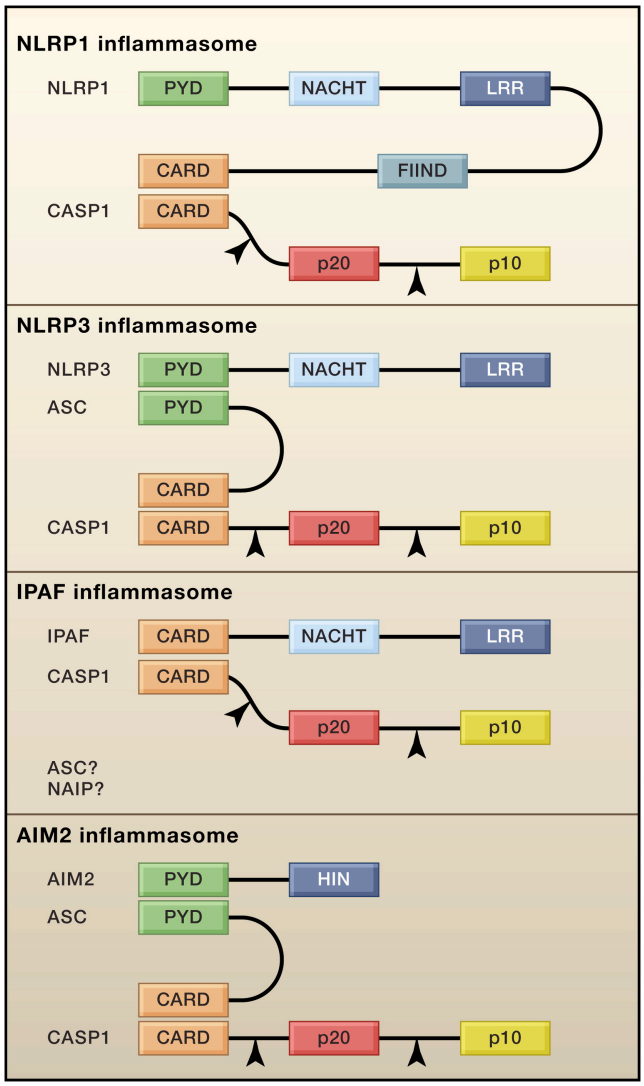

Figure 3. Constituents of unoligomerized inflammasomes. Processing of the caspase-1 by autocleavage at the sites indicated (black arrows), results in formation of the active caspase-1 p10/p20 tetramer. Domains: CARD, caspase recruitment domain; FIIND, domain with function to find; HIN, HIN-200/IF120x domain; LRR, leucine rich-repeat domain; NACHT, nucleotide-binding and oligomerization domain; PYD, pyrin domain [5].

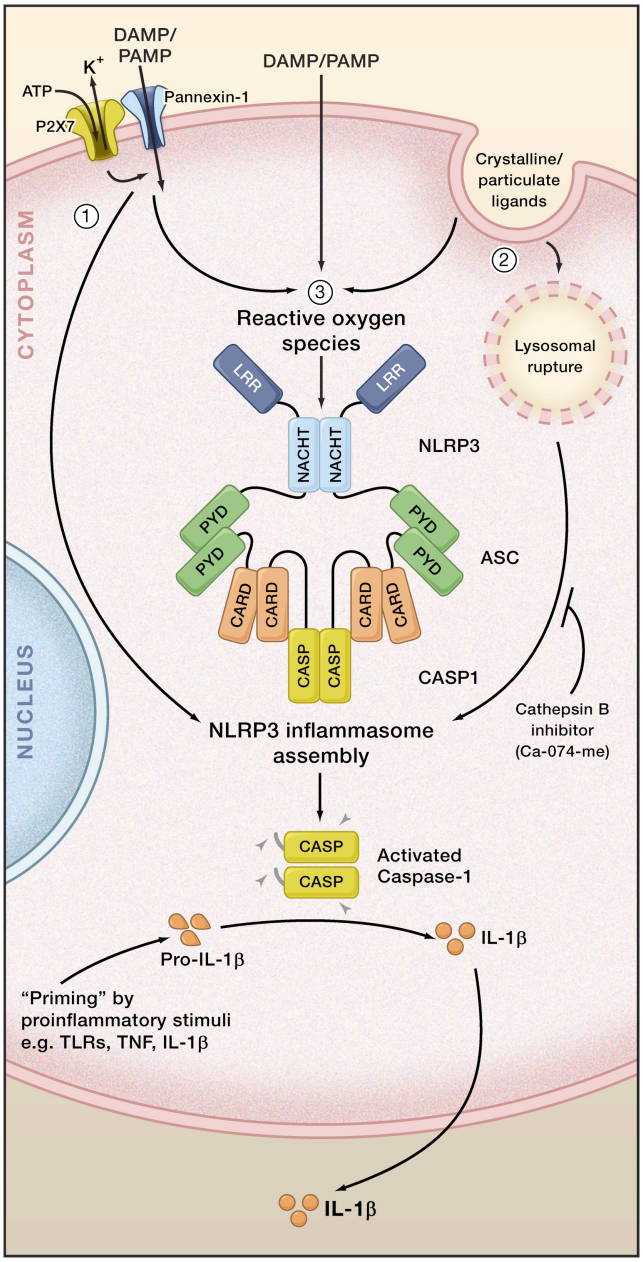

Figure 4. NLRP3 inflammasome activation. Three major models of inflammasome activation: (**1**) The NLRP3 agonist, ATP, triggers P2X7-dependent pore formation by the pannexin-1 hemichannel, allowing extracellular NLRP3 agonists to enter the cytosol and directly engage NLRP3. (**2**) Crystalline or particulate NLRP3 agonists are engulfed, and their physical characteristics lead to lysosomal rupture. The NLRP3 inflammasome senses lysosomal content in the cytoplasm, for example, via cathepsin-B-dependent processing of a direct NLRP3 ligand. (**3**) All danger-associated molecular patterns (DAMPs) and pathogen-associated molecular patterns (PAMPs), including ATP and particulate/crystalline activators, trigger the generation of reactive oxygen species (ROS). A ROS-dependent pathway triggers NLRP3 inflammasome complex formation. Caspase-1 clustering induces autoactivation and caspase-1-dependent maturation and secretion of proinflammatory cytokines, such as interleukin-1β (IL-1β) and IL-18 [5].

The main function of the NLRs has been indicated to be regulation of the pro-inflammatory cytokine production of cytokines interleukin-1 beta (IL-1β) and interleukin-18 (IL-18). Release of IL-1β is an important mediator of inflammation during infection [53]. Interleukins are a group of cytokines, or secreted signalling molecules, produced by a variety of cells. The interleukins promote development and differentiation of T, - B and hematopoetic cells, and are essential for both innate and adaptive immunity [54]. Due to possible detrimental effects of released IL-1β, the synthesis, processing and release is tightly controlled. The mechanisms involved in transcription of pro-IL-1β are now thought to involve signalling of nuclear factor kappa B (NFκB) and mitogen activated protein (MAP) kinases [55]. This signalling causes accumulation of intracellular stores of pro-IL-1β, and is followed by cleavage and release of the mature cytokine. The cleavage and release require to distinct stimuli. First an initial through innate PRRs, like the transmembrane TLR4, causes the accumulation. Second, cleavage is made possible by assembly of an inflammasome, like the NLRP3 inflammasome [54].

Caspases are cystein proteases that initiate or execute cellular programs, leading to inflammation or cell death. They are synthesized as inactive zymogens and controlled by proteolytic activation. Caspases are categorized as either pro-inflammatory or pro-apoptotic. The pro-inflammatory caspases are comprised of caspases-1, -11 and -12 in mice and caspase-1, -4, and -5 in humans [5, 56]. The catalytic activity of caspase-1 is regulated by signal-dependent auto activation within the inflammasome, which further results in processing of cytokines, like IL-1β [57].

Different models for activation of the NLRP3 inflammasome have been suggested. Three major models for activation will be described below, see also **Figure 4**. In the first model extracellular ATP stimulates the P2X7 ATP-gated ion-channel, triggering K^+ efflux, and inducing gradual recruitment of the pannexin-1 membrane pore. Formation of the pore allows extracellular DAMPs/PAMPs to access the cytosol and directly activate the NLRP3 inflammasome [58]. The second model proposes that engulfment of crystalline or particulate structures, such as silica and asbestos, by phagocytes leads to lysosomal damage. Lysosomal damage will further result in release of lysosomal contents that are sensed by the inflammasome as a DAMP [54,59]. The lysosomal protease, cathepsin B, was also suggested as a NLRP3 ligand by this mechanism. In the third model, all NLRP3 agonist trigger the generation of reactive oxygen species (ROS), and this common pathway triggers the inflammasome [60]. However, it is unclear how NLRP3 can detect such a diversity of stimuli, and there is no evidence that any ligands bind directly to the

complex. It has therefore been proposed an indirect activation, but this has yet to be determined [54].

Upon NLRP3 activation, the NLRP3 oligomerize which leads to clustering of the PYD domains of NLRP3 and the PYD domains of the adaptor ASC. In addition, the CARD domains of ASC will recruit the CARD domains of pro-caspase-1. Clustering of pro-caspase-1 allows for autocleavage and formation of the active units of caspase-1, namely the p10/p20 tetramer. Activated caspase-1 is then able to process proforms of cytokines IL-1β and IL-18 and generate active molecules for secretion [5], **Figure 4**.

References:

1. Pestka, J. and H.-R. Zhou, *Toll-Like Receptor Priming Sensitizes Macrophages to Proinflammatory Cytokine Gene Induction by Deoxynivalenol and Other Toxicants.* Toxicological Sciences, 2006. **92**(2): p. 445-455.
2. Kankkunen, P., et al., *Trichothecene Mycotoxins Activate Inflammatory Response in Human Macrophages.* The Journal of Immunology, 2009. **182**(10): p. 6418-6425.
3. Vermeulen, K., D.R. Van Bockstaele, and Z.N. Berneman, *The cell cycle: a review of regulation, deregulation and therapeutic targets in cancer.* Cell Proliferation, 2003. **36**(3): p. 131-149.
4. Fink, S.L. and B.T. Cookson, *Apoptosis, Pyroptosis, and Necrosis: Mechanistic Description of Dead and Dying Eukaryotic Cells.* Infect. Immun., 2005. **73**(4): p. 1907-1916.
5. Schroder, K. and J. Tschopp, *The Inflammasomes.* Cell, 2010. **140**(6): p. 821-832.
6. CAST (Council for Agricultural Science and Technology, A., Iowa.), *Mycotoxins: Risks in plant, animal and human systems — Task force report No. 139/January 2003.* 2003.
7. Windels, C.E., *Economic and Social Impacts of Fusarium Head Blight: Changing Farms and Rural Communities in the Northern Great Plains.* Phytopathology, 2000. **90**(1): p. 17-21.
8. Jestoi, M., *Emerging Fusarium-Mycotoxins Fusaproliferin, Beauvericin, Enniatins, And Moniliformin—A Review.* Critical Reviews in Food Science and Nutrition, 2008. **48**(1): p. 21 - 49.
9. Bottalico, A., *Fusarium diseases of cereals: Species complex and related mycotoxin profiles in Europe.* Journal of Plant Pathology, 1998. **80**: p. 85-103.
10. Jestoi, M., et al., *Presence and concentrations of the Fusarium-related mycotoxins beauvericin, enniatins and moniliformin in finnish grain samples.* Food Additives and Contaminants, 2004. **21**(8): p. 794 - 802.
11. Melino, G., *The Sirens' song.* Nature, 2001. **412**(6842): p. 23-23.
12. Kroemer, G., et al., *Classification of cell death: recommendations of the Nomenclature Committee on Cell Death 2009.* Cell Death Differ, 2009. **16**(1): p. 3-11.
13. Kerr, J.F., A.H. Wyllie, and A.R. Currie, *Apoptosis: A Basic Biological Phenomenon with Wide-ranging Implications in Tissue Kinetics.* British Journal of Cancer, 1972. **26**: p. 239-257.

14. Baehrecke, E.H., *How death shapes life during development.* Nat Rev Mol Cell Biol, 2002. **3**(10): p. 779-787.
15. Jacobson, M.D., M. Weil, and M.C. Raff, *Programmed Cell Death in Animal Development.* Cell, 1997. **88**(3): p. 347-354.
16. Tang, P.S., et al., *Acute lung injury and cell death: how many ways can cells die?* American Journal of Physiology - Lung Cellular and Molecular Physiology, 2008. **294**(4): p. L632-L641.
17. Leist, M. and M. Jäättelä, *Four deaths and a funeral: from caspases to alternative mechanisms.* Nat Rev Mol Cell Biol, 2001. **2**(8): p. 589-598.
18. Vaculova, A. and B. Zhivotovsky, *Caspases: determination of their activities in apoptotic cells.* Methods in Enzymology, 2008. **442**: p. 157-181.
19. Orrenius, S., P. Nicotera, and B. Zhivotovsky, *Cell Death Mechanisms and Their Implications in Toxicology.* Toxicological Sciences, 2011. **119**(1): p. 3-19.
20. Danial, N.N. and S.J. Korsmeyer, *Cell Death: Critical Control Points.* Cell, 2004. **116**(2): p. 205-219.
21. Kroemer, G. and S.J. Martin, *Caspase-independent cell death.* Nat Med, 2005. **11**(7): p. 725-730.
22. Green, D.R. and G. Kroemer, *The Pathophysiology of Mitochondrial Cell Death.* Science, 2004. **305**(5684): p. 626-629.
23. Chipuk, J.E. and D.R. Green, *Do inducers of apoptosis trigger caspase-independent cell death?* Nat Rev Mol Cell Biol, 2005. **6**(3): p. 268-275.
24. Cookson, B.T. and M.A. Brennan, *Pro-inflammatory programmed cell death.* Trends in Microbiology, 2001. **9**(3): p. 113-114.
25. Mariathasan, S., et al., *Differential activation of the inflammasome by caspase-1 adaptors ASC and Ipaf.* Nature, 2004. **430**(6996): p. 213-218.
26. Willingham, S.B., et al., *Microbial Pathogen-Induced Necrotic Cell Death Mediated by the Inflammasome Components CIAS1/Cryopyrin/NLRP3 and ASC.* Cell Host & Microbe, 2007. **2**(3): p. 147-159.
27. Labbe, K. and M. Saleh, *Cell death in the host response to infection.* Cell Death Differ, 2008. **15**(9): p. 1339-1349.
28. Klionsky, D.J. and S.D. Emr, *Autophagy as a Regulated Pathway of Cellular Degradation.* Science, 2000. **290**(5497): p. 1717-1721.
29. Levine, B. and V. Deretic, *Unveiling the roles of autophagy in innate and adaptive immunity.* Nat Rev Immunol, 2007. **7**(10): p. 767-777.

30. Bartek, J. and J. Lukas, *Mammalian G1- and S-phase checkpoints in response to DNA damage.* Current Opinion in Cell Biology, 2001. **13**(6): p. 738-747.
31. Ljungman, M., *Activation of DNA damage signaling.* Mutation Research/Fundamental and Molecular Mechanisms of Mutagenesis, 2005. **577**(1-2): p. 203-216.
32. Harper, J.W. and S.J. Elledge, *The DNA Damage Response: Ten Years After.* Molecular Cell, 2007. **28**(5): p. 739-745.
33. Smith, J., et al., *The ATM-Chk2 and ATR-Chk1 pathways in DNA damage signaling and cancer.* Adv Cancer Res, 2010. **108**(73-112).
34. Pestell, R.G., et al., *The Cyclins and Cyclin-Dependent Kinase Inhibitors in Hormonal Regulation of Proliferation and Differentiation.* Endocrine Reviews, 1999. **20**(4): p. 501-534.
35. Wang, Y. and C. Prives, *Increased and altered DNA binding of human p53 by S and G2/M but not Gl cyclin-dependent kinases.* Nature, 1995. **376**(6535): p. 88-91.
36. Norbury, C. and P. Nurse, *Animal Cell Cycles and Their Control.* Annual Review of Biochemistry, 1992. **61**(1): p. 441-468.
37. Pines, J., *Cyclins: wheels within wheels.* Cell Growth Differ, 1991. **2**(6): p. 305-310.
38. Assoian, R.K. and X. Zhu, *Cell anchorage and the cytoskeleton as partners in growth factor dependent cell cycle progression.* Current Opinion in Cell Biology, 1997. **9**(1): p. 93-98.
39. Ohtsubo, M., et al., *Human cyclin E, a nuclear protein essential for the G1-to-S phase transition.* Mol. Cell. Biol., 1995. **15**(5): p. 2612-2624.
40. Girard, F., et al., *Cyclin a is required for the onset of DNA replication in mammalian fibroblasts.* Cell, 1991. **67**(6): p. 1169-1179.
41. Arellano, M. and S. Moreno, *Regulation of CDK/cyclin complexes during the cell cycle.* The International Journal of Biochemistry & Cell Biology, 1997. **29**(4): p. 559-573.
42. Sherr, C.J. and J.M. Roberts, *Inhibitors of mammalian G1 cyclin-dependent kinases.* Genes & Development, 1995. **9**(10): p. 1149-1163.
43. Lloyd, R.V., et al., *p27kip1: A Multifunctional Cyclin-Dependent Kinase Inhibitor with Prognostic Significance in Human Cancers.* The American Journal of Pathology, 1999. **154**(2): p. 313-323.
44. Pan, Z.-Q., et al., *Inhibition of Nucleotide Excision Repair by the Cyclin-dependent Kinase Inhibitor p21.* Journal of Biological Chemistry, 1995. **270**(37): p. 22008-22016.
45. Matzinger, P., *Tolerance, Danger, and the Extended Family.* Annual Review of Immunology, 1994. **12**(1): p. 991-1045.

46. Takeda, K. and S. Akira, *Toll-like receptors in innate immunity.* International Immunology, 2005. **17**(1): p. 1-14.
47. Huysamen, C. and G.D. Brown, *The fungal pattern recognition receptor, Dectin-1, and the associated cluster of C-type lectin-like receptors.* FEMS Microbiology Letters, 2009. **290**(2): p. 121-128.
48. Yoneyama, M. and T. Fujita, *RIG-I family RNA helicases: Cytoplasmic sensor for antiviral innate immunity.* Cytokine & Growth Factor Reviews, 2007. **18**(5-6): p. 545-551.
49. Takaoka, A. and T. Taniguchi, *Cytosolic DNA recognition for triggering innate immune responses.* Advanced Drug Delivery Reviews, 2008. **60**(7): p. 847-857.
50. Hornung, V., et al., *AIM2 recognizes cytosolic dsDNA and forms a caspase-1-activating inflammasome with ASC.* Nature, 2009. **458**(7237): p. 514-518.
51. Martinon, F., A. Mayor, and J. Tschopp, *The Inflammasomes: Guardians of the Body.* Annual Review of Immunology, 2009. **27**(1): p. 229-265.
52. Kono, H. and K.L. Rock, *How dying cells alert the immune system to danger.* Nat Rev Immunol, 2008. **8**(4): p. 279-289.
53. Dinarello, C.A., *Interleukin-1beta.* Critical Care Medicine, 2005. **33**(12): p. 460-462.
54. Bryant, C. and K.A. Fitzgerald, *Molecular mechanisms involved in inflammasome activation.* Trends in Cell Biology, 2009. **19**(9): p. 455-464.
55. Hiscott, J., et al., *Characterization of a functional NF-kappa B site in the human interleukin 1 beta promoter: evidence for a positive autoregulatory loop.* Mol. Cell. Biol., 1993. **13**(10): p. 6231-6240.
56. Martinon, F. and J. Tschopp, *Inflammatory caspases and inflammasomes: master switches of inflammation.* Cell Death Differ, 2006. **14**(1): p. 10-22.
57. Martinon, F., K. Burns, and J. Tschopp, *The Inflammasome: A Molecular Platform Triggering Activation of Inflammatory Caspases and Processing of proIL-[beta].* Molecular Cell, 2002. **10**(2): p. 417-426.
58. Kanneganti, T.-D., et al., *Pannexin-1-Mediated Recognition of Bacterial Molecules Activates the Cryopyrin Inflammasome Independent of Toll-like Receptor Signaling.* Immunity, 2007. **26**(4): p. 433-443.
59. Hornung, V., et al., *Silica crystals and aluminum salts activate the NALP3 inflammasome through phagosomal destabilization.* Nat Immunol, 2008. **9**(8): p. 847-856.
60. Cassel, S.L., et al., *The Nalp3 inflammasome is essential for the development of silicosis.* Proceedings of the National Academy of Sciences, 2008. **105**(26): p. 9035-9040.

Figure references:

Figure 1: Fink, S.L. and B.T. Cookson, *Apoptosis, Pyroptosis, and Necrosis: Mechanistic Description of Dead and Dying Eukaryotic Cells.* Infect. Immun., 2005. **73**(4): p. 1907-1916.

Figure 2: Vermeulen, K., D.R. Van Bockstaele, and Z.N. Berneman, *The cell cycle: a review of regulation, deregulation and therapeutic targets in cancer.* Cell Proliferation, 2003. **36**(3): p. 131-149.

Figure 3: Schroder, K. and J. Tschopp, *The Inflammasomes.* Cell, 2010. **140**(6): p. 821-832.

Figure 4: Schroder, K. and J. Tschopp, *The Inflammasomes.* Cell, 2010. **140**(6): p. 821-832.

Enniatin B induced inflammatory response and cell death in RAW 267.4 murine macrophages

Authors:

A. Gammelsrud[1], A. Solhaug[1], W. Sandberg[2], L. Ivanova[1], B Dendelé[3], **A. Bølling[2], M.Refsnes[2], R.Becher[2],** D Lagadic-Gossmann[3] **G. Eriksen[1], J. A. Holme[2]**

Affiliation:

[1]*Section for Chemistry and Toxicology, Norwegian Veterinary Insitute, P.O. Box 750, Sentrum, N-0106 Oslo, Norway.*
[2]*Department of Air Pollution and Noise, Division of Environmental Medicine, Norwegian Institute of Public Health, N-0403 Oslo, Norway.*
[3]*Inserm U620, Université Rennes*

Corresponding author:
Dr. Jørn A. Holme
Department of Air Pollution and Noise,
Division of Environmental Medicine
Norwegian Institute of Public Health
P. O. Box 4404 Nydalen
N-0403 Oslo, Norway
E-mail: jorn.holme@fhi.no
Phone: +47 2076247
Fax: +47 21076686

KEYWORDS: Mycotoxins, Enniatins, cytokines, inflammasome, apoptosis,

Abbreviations

AB, Alamar blue;

ASC, Apoptotic speck protein containing a C-terminal caspase recruitment domain;

CDK, Cyclin dependent kinase;

CDKI, Cyclin dependent kinase inhibitor;

Ctx B, Cholera toxin subunit B;

DAMP, Danger associated molecular patterns;

EnnB, Enniatin B;

NR, Neutral red;

PAMP, Pathogen associated molecular pattern;

PI, Propidium Iodide;

PRR, Pattern recognition receptor;

TLR, Toll-like receptor;

ZYVAD-FMK, Z-VAD-fmk, *N*-benzyloxycarbonyl-Val-Ala-Asp-fluoromethylketone;

Abstract

The mycotoxin enniatin B (EnnB) is predominantly produced by species of the *Fusarium* genera, and is one of the emerging Fusarium mycotoxins reported to be found at high concentrations in Norwegian grain. The cytotoxic effect of EnnB is thought to be caused by the ability to form ionophores in cellular lipid membranes. In the present study, RAW 264.7 macrophages of mouse origin were exposed to EnnB followed by the use of different assays in order to characterize the effect on cell death, cell proliferation, differentiation and potential inflammatory response. Exposure to EnnB arrested the cells in the G_1-phase of the cell cycle after 24 hr exposure, and induced morphological features related to apoptosis in cells examined by fluorescence microscope. Damaged lyosomes were also observed on micrographs. Elevated levels of activated caspase-1 were observed after exposure, and cells primed with lipopolysaccharide (LPS) in addition to EnnB secreted significantly higher levels of interleukin-1 beta (IL-1β), compared to the controls. Treatment with the caspase-1 specific inhibitor, ZYVAD-FMK, prior to exposure with both LPS and EnnB inhibited this cytokine release. Activation of the inflammasome, followed by cleavage of caspase-1 and processing and release of IL-1β is proposed as a mechanism of action for EnnB.

Introduction

Enniatin B (EnnB) is a mycotoxin/secondary metabolite produced predominantly by species of the *Fusarium* genera [1]. The enniatins belong to a group of cyclohexadepsipeptides, and are commonly composed of three D-α-hydroxyvaleric acids linked with three L-configured N-methyl amino acids joined together in a ring by peptide and ester bonds (*for EnnB*, **fig. 1**). The lipophilic nature of enniatins might therefore lead to accumulation in animal tissue. [2]. The molecular weight of EnnB is 639 [3].

Grain in Northern Europe is found to be contaminated with the enniatin producing fungus *Fusarium Avenaceum* in high numbers, and field studies have shown that the field conditions in Scandinavia seem to favour enniatin production [4]. In Norwegian grain samples it has been reported enniatin concentrations of up to several mg/kg [5], and even higher concentrations have been found in analysis of Finnish grains. EnnB has been present in 99% of the different grain samples reported by studies in Finland, Norway, and Italy [4]. *F. avenaceum* is also known to produce other mycotoxins in addition to enniatins, namely beauvericin (BEA) and moniliformin (MON) [4].

Enniatins have been reported to have a wide range of effects *in vitro*, and have been described to have ionophoric, phytotoxic, insecticidal, and antibacterial properties [1]. At physiological ion concentrations, the primary mechanism triggering toxicity is its effects as an ionophore, by forming channels in cellular lipid membranes [6, 7]. Both mono-and divalent cations are affected, with the effects on K^+ and Ca^{2+} being the most described [8]. In addition to inhibition of acyl-COA:cholesterol acyltransferase (ACAT) activity [9], the hypolipidaemic action of EnnB is thought to be caused by a reducation of triglyceride synthesis and diminishing of the free fatty acid pool in the cells [10]. Studies have also shown enniatins to have toxic effects on several cancer cell lines, and they are considered used as anti cancer drugs [11,12]. Additional studies have shown enniatins to interact with the multidrug protein Pdr5p in *Saccharomyces cerevisiae* at non-toxic concentrations, and with the human P-glycoprotein (Pgp) in MRP2 and BCRP [13-15].

Data from *in vivo* studies of enniatins is sparse, with only one report of *in vivo* toxicity caused by the effects of enniatins [16-18]. However, since contamination in cereals is found and enniatins

are co-occurring with other mycotoxins, especially deoxynivalenol (DON) and MON, further research is needed.

Innate immunity, the first line of defence against pathogens, is in part activated via Toll-like receptors (TLRs), which recognize pathogen-associated molecular patterns (PAMPs) [19]. Lipopolysaccharide (LPS), a component of the gram-negative bacterial cell wall, is principal in the role of inflammatory responses [20]. In response to LPS stimulation via TLR4, mononuclear phagocytes produce proinflammatory cytokines (e.g. IL-1 and TNf-α), bioactive lipids (e.g. prostaglandins), and reactive oxygen species. It has been shown that the toxicity of other mycotoxins like DON and T-2 (type A trichothecene) have been potentiated by priming (pre-treatment) with LPS [21, 22].

Enniatins have in other studies been indicated to exert their cytotoxic activities, in addition to being ionophores, through the induction of mitochondrial modifications and cell cycle disruption, resulting in apoptotic cell death [11, 12, 23]. The apoptotic cell death is reportedly not induced by generation of reactive oxygen species (ROS) or by damaging the DNA [11]. The morphological features of apoptosis observed after exposure to enniatins are chromatin condensation and formation of apoptotic bodies. Other apoptotic features are reduction of cellular and nuclear volume, DNA-fragmentation, and exposure of phosphatidylserine on the extracellular side of the plasma membrane. Related to the effects on the cell cycle, enniatins have been described to induce a cell cycle arrest in the G_0/G_1 phase by activation of early working cell cycle inhibitors [11].

The aim of this study was to characterize the effects of EnnB on cell death, cell proliferation differentiation and potential inflammatory effects in RAW 264.7 machrophages of mouse origin.

Materials and methods

Reagents and chemicals

EnnB was purified from *F.avenaceum* cultures as described in Ivanova et al. [3], Alamar Blue were from Biosource (Nivelles, Belgum), the Neutral Red kit from Xenometrix (Allschwil, Switzerland) the Annexin V kit from BD Biosciences Pharmingen (San Diego, CA, USA), the Tunel Assay (In Situ Cell Death Detection Kit, TMR red) were from Roche Diagnostics (Indianapolis, Indiana, USA) and the IL-1beta ELISA kit were from R&D Systems (Minneapolis, Minnesota 55413, USA) (Mouse IL-1 beta/IL-1F2 DuoSet, DY401, LOT 1210432). Propidium iodide (PI, 1.0 mg/mL), Hoechst 33342 (10 mg/mL), DAPI, Cholera toxin subunit B (recombinant) Alexa Fluor 488 conjugate, RNAse (Purelink™ RNase A), LMPA (low melting point agarose) and NMPA (Normal melting point agarose), Bovin Serum Albumin (BSA) were purchased from Invitrogen. Gels and buffers for Western blotting (NuPAGE system) were all purchased from Invitorgen. FPG (formamidopyrimidine DNA glycosylase) was kindly provided by Andrew Collins (University of Oslo, Norway).

The Caspase-1 inhibitor ZYVAD-FMK were from EMD Chemicals, Inc., (Gibbstown, USA), Dimethyl sulfoxide (DMSO), Lipopolysaccharide (LPS from *E. coli* O26:B6), Triton X-100, Paraformaldehyde were purchased from Sigma-Aldrich Chemical Company (St Louis, MO, USA), Silica nano particles (amorphous, monodisperse, d=100 nm) from Kisker Biotech (Steinfurt, Germany), Lysisbuffer (#9803) from Cell Signaling, Dulbecco's Modified Eagle Medium (DMEM), Penicillin/Streptomycin and Fetal bovine serum (FBS) were from Lonza (Verviers, Belgium), Bio-RAD DC protein assay from Bio-Rad Laboratories Inc (Hercules, CA). All other chemicals were purchased from commercial sources and were of analytical grade.

Antibodies

P27 Kip1 (#3698), phospho-p53 (ser15) (#9284), phospho-p53 (ser392) (#9281),Phospho-Histone H2A.X (Ser139) –Alexa Fluor 488 conjugate (#9719), Phospho-NF-κB p65 (Ser536) – Alexa Flour 488 conjugate (4886), Cleaved Caspase 3 (#9661), Cyclin D1 (#2922), Cyclin E (#4129), Caspase 1 (#2225), IkBα (#9242), β-Actin Rabbit mAb HRP Conjugate (#5125), Anti-Mouse IgG HRP-linked Anti body (#7076), Anti-Rabbit IgG HRP-linked Antibody (#7074) were purchased from Cell Signaling (Beverly, MA, USA). p21 Alexa Flour conjugate (#sc-6246), CD163 (K-18; #sc-18796) were from Santa Cruz Biotecnology (Santa Cruz, CA, USA) anti-rabbit Alexa Flour 488, anti-rabbit Alexa Flour 647 and anti-goat Alexa Flour 488 were from Molecular Probes, (Eugene, OR, USA).

Cell Culture and Treatments

Both the murine macrophage cell line RAW264.7 and J774A.1 was obtained from European Collection of Cell Culture (ECACC) and grown in DMEM containing 4,5 g/L glucose supplemented with 10% heat inactivated FBS penicillin (100 U/ml), and streptomycin (100 μg/ml). The cells were cultured at 37°C under 5% CO_2 in a humidified incubator and routinely kept in logarithmic growth phase at 3 x 10^6 – 20 x 10^6 cells/75 cm^2 by splitting the cells by scraping twice a week. Fresh medium was added before scraping. The passage number was kept below 25.

If not otherwise stated, the cells were seeded at a density of 35 000 cells/cm^2 and allowed to adhere over night before exposure. In experimental setups were the integrity of the plasma membrane and plasma membrane associated proteins (annexin V, CD163) were important, UpCell™ cell culture dishes were used. The surface of these dishes is temperature responsive and allows cells to detach without the use of cell scrapers in temperatures below 32°C. For harvesting, the dishes were therefore put on ice for 10 min to allow the cells to detach.

For treatment with ZYVAD-FMK, a specific caspase-1 inhibitor [24], the cell culture medium was replaced with fresh medium containing the inhibitor. The cells were pre-incubated with the inhibitor for 30 min, followed by the treatment with EnnB at the concentrations and time points as indicated. EnnB were dissolved in DMSO and the final concentration of DMSO in the cell

cultures was 0,1%. Appropriate controls containing the same amount of solvent were included in each experiment. These controls will be referred to as DMSO or simply controls. This experimental setup was used if nothing else is described.

Cell viability

Following EnnB exposure, the metabolic activity of the RAW 264.7 cells was measured using alamar blue assay according to manufacturer (Biosource, Nivelles, Belgium). The dark blue oxidized form of alamar blue, resazurin, has little fluorescence. When taken into cells resazurin is reduced to resorifon, which is highly fluorescent. This reaction occurs in cells with actively working mitochondria [25] and the measured fluorescence intensity is proportional to number of cells. The fluorescence (585 nm) of resorufin was quantified using a Victor^2 Multilabel Counter (PerkinElmer, Boston, MA, USA).

Cell viability of the Raw 264.7 cells was also measured with a neutral red (NR) assay, which is a colormetric assay for the quantification of membrane permeability and lysosomal activity in the cells. Measurements were done according to the manufacturer's procedure (Xenometrix, Allschwil, Switzerland). The NR assay is based on the ability of viable cells to incorporate and bind NR within lysosomes. The quantity of dye incorporated into cells is directly proportional to the number of cells with an intact lysosomal membrane. The absorbance of NR (540 nm) was measured using a Victor2 Multilabel Counter (PerkinElmer, Boston, MA, USA).

Cell death observed with microscopy

Changes in nuclear morphology and plasma membrane damages were evaluated after staining cells (~0,5 x 10^6 cells) with PI (10 μg/ml) and Hoechst 33342 (5 μg/ml) for 30 min. Stained cells suspended in FBS were smeared on slides and air dried quickly. Nuclear morphology associated with necrosis and apoptosis were determined using a Nikon Eclipse E400 fluorescence microscope. Cells with distinct condensed nuclei, segregated nuclei, and apoptotic bodies were counted as apoptotic, and cells with half-condensed "donut-like" nucleus were counted as early apoptotic (apo*). Non-apoptotic cells, excluding PI, were categorized as viable cells. And cells with an increased cellular volume, stained with PI were termed necrotic. The fraction of cells in

each category was compared to the total number of cells. A minimum of 300 cells per slide were counted.

Changes in cell morphology observed with microscopy

The cells were seeded and exposed as described above. 300 cells in 5 sectors of each cell culture dish were counted using a light microscopy (Leica DMIL), and the fraction of elongated cells was compared to the total number of counted cells. Pictures were taken with a Moticam 1000.

Cell Cycle analysis by flow cytometry

Following drug exposure the cells were harvested by scraping, washed with PBS and fixed with ice-cold 70% EtOH over night at -20°C. The cells were then incubated with PI (10 µg/ml) and RNase A (100 µg/ml) in PBS for 30 min at 37°C before analysis on a flow cytometer, Accuri C6 or LSRII (BD). Single cells were gated and a minimum of 10 000 events were analyzed in each sample. The percentages of cells in the different phases of the cell cycle as well as apoptotic cells were estimated from DNA histogram using the Multicycle Program (Phoenix Flow system, San Diego, CA, USA). Apoptotic index was determined as the percentage of signals between the G_1 peak and the channel positioned at 20% of the G_1 peak, Sub-G_1.

Measurement of apoptosis by flow cytometry

In early apoptotic cells, the membrane of phospholipids phosphatidylserine (PS) is translocated from the inner to the outer leaflet of the plasma membrane, thereby exposing phosphatidylserine (PS) to the extracellular environment [26]. Annexin V is a Ca^{2+} dependent phospholipid-binding protein with high affinity for PS. Annexin V will bind to cells exposing PS to the extracellular side of the plasma membrane. Annexin V coupled to FITC in combination with PI, which is excluded by viable cells, is used as staining to determine different phases of apoptosis. Cells considered as viable are both annexin V FITC and PI negative, early apoptotic cells are annexin V FITC positive and PI negative, late apoptotic or necrotic cells are both annexin V and PI positive. For the annexin V asay, the cells were plated on UpCell™ plates (Nunc) and exposed to

EnnB as described above. Exposed cells were harvested and washed twice in cold PBS, and 1 x 10^5 cells were stained and incubated according to the procedure described by the manufacturer of the FITC Annexin V apoptosis detection kit I (BD Biosciences, San Diego, CA, USA). The cells were then analyzed by flow cytometry with a LSRII (BD Biosciences) or an Accuri C6.

One of the later steps in apoptosis is DNA fragmentation, a process which results from the activation of endonucleases during the apoptotic program. Those DNA strand breaks can be detected by enzymatic labelling of the 3`-OH termini with modified nucleotides. This end-labelling method has been termed the TUNEL (Terminal deoxynucleotidyl transferase dUTP nick end labelling) Assay. For the TUNEL assay, the cells were harvested by scraping, washed once in PBS, fixed in 1% PFA in PBS 15 min on ice, and post-fixed/permeabilized in 90% ice cold methanol for at least 2 days at -20°C. DNA fragmentation were then identified by using the TUNEL Assay (In Situ Cell Death Detection Kit, TMR red, from Roche Diagnostics) according to the procedure described by the manufacturer.

Measurement of surface proteins, CD163 by flow cytometry

CD163 is a transmembrane protein found exclusively on macrophages and monocytes, and is a marker of activated macrophages, type M2 [27]. The cells were plated on UpCell™ plates (Nunc) and exposed to EnnB as described above. Harvested cells were then washed once in 5% BSA/PBS, 6 x 10^5 cells were incubated with CD163 antibody in the dark for 1 hr, washed twice in 0,5% BSA/PBS, and incubated with secondary antibody, a-goat Alexa Flour 488 for 30 min. The cells were then washed twice in in 0,5% BSA/PBS, resuspended in PBS and analyzed with a flow cytometer, Accuri C6. Single cells were gated and a minimum of 10 000 cells were analyzed.

Measurement of intracellular proteins by flow cytometry

The cells were harvested, washed once in PBS, fixed in 1% PFA in PBS on ice for 15 min, and post-fixed/permeabilizated in 90% ice cold methanol for at least 2 days at -20°C. For staining with antibody, 5 x 10^5 cells were washed two times in 5% BSA in PBS and incubated with primary antibody or direct conjugated antibody in 5% BSA/PBS/0.2% Triton X-100 overnight at

4°C or 30 min - 2 hrs at room temperature. If direct conjugated antibodies not were used, the cells were rinsed twice in 5% BSA/PBS/0.2% Triton X-100 and incubated with secondary antibody conjugated to Alexa Fluor 488 for 2 hrs at room temperature in the dark. The cells were then analyzed with an Accuri C6 or a LSRII (BD) flow cytometer. Single cells were gated and a minimum of 10 000 cells were acquired and analyzed.

Western Blotting

Differences in expression of cellular proteins were compared by Western immunoblot analysis. After exposure the cells were washed twice in ice-cold PBS and placed at -70°C for a minimum of 24 hrs, treated with lysis buffer (Cell signalling), and centrifuged at 14000 x g. Protein concentration of the supernatant was measured using a Bio-RAD DC protein assay kit, and the protein concentrations of the samples were equally adjusted by adding lysis buffer. The Western blotting was performed using Invitrogen NuPage Novex Bis-Tris gels according to the procedure described by the manufacturer (Invitrogen). After blotting membranes were stained with Ponceau S dye, and blots with equal protein loading were used. The membranes were then blocked with 5% non-fat milk in Tris Buffered Saline (TBS) or 5% BSA in TBS for 30 min, and incubated with primary antibodies over night at 4°C (or 3 hrs at room temperature. The primary antibodies were diluted in either 5% BSA in TBS-Tween (TBST) or 5% non-fat milk in TBST. Incubation was followed by washing of the blots in TBST, and incubating with secondary HRP-conjugated antibodies diluted in incubation buffer for 1 hr. After incubation with secondary antibodies the membranes were again washed, and immunoreactive proteins were detected using a chemiluminescence system according to the manufacturer's instructions (Super signal west dura chemoluminiscence system, Thermo Scientific, IL). Pictures were taken with a ChemiDoc XRS+ (Bio-Rad), and images analyzed with Image Lab 3.0 (Bio-Rad Laboratories, California, USA).

Immunocytochemistry

To investigate presence of proteins associated with elongation (differentiation) cells were stained with antibodies for CD163 after 6 hr EnnB and DMSO exposure. Exposed cells were washed with PBS and fixed in methanol for 3 min before over night incubation with primary antibody, polyclonal goat anti-CD163 (working dilution of 1:50 and 1:100) at room temperature. After

washing and incubation with anti-goat Alexa Flour 488 conjugated antibody for 3 hrs, the preparations were mounted and visualized using a Nikon Eclipse E400 microscope and a SPOT diagnostic instruments digital camera. As controls, the secondary antibody was omitted (not shown).

Alkaline Comet Assay

The comet assay was essentially performed as described previously by Collins et al. [28]. Brifely, the cells were resuspended in 75 µl 1% low melting point agarose at 37°C, applied onto glass slides (pre-coated with 1% normal melting point agarose and dried), and covered with cover slips. Two equal gels were made on each slide. The slides were placed at 4°C for 10 min to allow the gel to set, then immersed in pre-chilled lysis buffer (2,5 M NaCl, 0,1 M EDTA, 10 mM Tris-HCl, pH 10, 1% Triton X-100) and incubated at 4°C for 1 hrs. The slides were then washed three times in washing-buffer (40 mM HEPES, 0,1 M KCl, 0,5 mM EDTA, 0,2 mg/ml BSA pH 8) at 4°C 5 min. One of the two gels at each slide were treated with formamidopyrimidineglycosylase (fpg; 1:3000), and the other gel was treated with washing buffer only, for 30 min, 37°C in a humidity chamber. After enzyme treatment the slides were immersed in a cold alkali solution (0,3 M NaOH, 1 mM EDTA pH>13) for 30 min following electrophoresis in a pre-chilled alkali solution (0,3 M NaOH, 1 mM EDTA pH>13) on 1V/cm 30 min and air-dried on the bench. The slides were stained with SYBR green (1:10 000) for 10 min and images were visualized under a fluorescence microscope (Olympus BX51, Olympus Europe, Hamburg, Germany) and acquired with a Olympus DP70 camera. A minimum of 100 comets each slides were analyzed using the TriTek CometScore™ Freeware (www.tritekcorp.com). The differences in tail intensity between Fpg-treated cells (total DNA damage) an untreated cells (basic DNA damage) were considered as 8-oxodGuo (oxidative DNA damage) in a single cell.

GM1 Immunofluorescence assay

GM1 is a type of ganglioside found in the plasma membrane and acts as the site of binding for cholera toxin. Cells were fixed for 30 min at 4°C with 4% PFA in PBS. After washing, the cells were incubated for 1 hr with blocking solution (2% BSA in PBS), followed by FITC-coupled choleratoxin (Ctx) B (Invitrogen) (0.5 µg/ml) for 1 hr. Pictures of fluorescent-labelled cells were

captured with a DMRXA Leica microscope and a COHU high performance CCD camera using Metavue software. In a variation of the assay described above, the cells were let to incubate with FITCH-coupled Ctx B for 2 hrs before fixation in order to observe any potential effect of EnnB.

Cytokine Measurement, ELISA

Secreted cytokines were measured with the enzyme linked immunosorbent assay (ELISA). The cells were plated in 24-well plates with a density of $4x10^5$ cells/well (~135 000/cm^2). All cells were let to adhere overnight, and fresh medium were added before Lipopolysaccaride (LPS) priming. A 3 hour LPS priming was followed by a 6 hour EnnB or DMSO exposure. The medium was then harvested and centrifuged (300 x g, 4°C, 10 min) to remove cell debris and the supernatant stored at -70 °C until use. Levels of IL-1β in cell medium were measured by ELISA Duoset (R&D systems, Minneapolis MN, USA) according to the manufacturers' guidelines. The absorbance levels were measured and quantified using a plate reader (TECAN Sunrise, Phoenix Research Products, Hayward, CA, USA) equipped with analyzing software (Magellan VI).

Electron Microscopy

The cells were fixed by drop-wise addition of glutaraldehyde and analysed according to standard conditions. After fixation, the specimens were made as described by Asare et al.[29]. Briefly the specimens were rinsed with PBS, followed by post-fixation with 1% osmium tetroxide in phosphate buffer for 1 hr. After further rinsing with PBS for 15 min, the specimens were dehydrated through a series of graded ethyl alcohols from 70% to 100%. Cells were then embedded in DMP30 Eponate for 2 days at 37°C and then for 24 hrs at 60°C. Thin sections (70 nm) were collected onto copper grids and counterstained with lead citrate before examination with a Philips transmission electron microscope.

Statistical analysis

The unpaired t-test was used for statistically comparison of two groups, and the data was assumed to follow a Gaussian distribution. The compared results are presented as mean ± SEM, and the probability values were considered significant when $p<0,05$. The p values of $<0,05$, $<0,01$, and $<0,0001$ are represented as *, **, and *** , respectively. Graphpad Prism 5.0 was used for all calculations.

Results

Cell viability and Cell death

By using the alamar blue (AB) and neutral red (NR) assay the cell viability of Raw 264.7 cells exposed of EnnB was measured compared to control (**fig. 2A and 3B**). Both assays are product of cell proliferation and cell function. With AB more specifically the mitochondrial metabolic activity is assessed [25], while the NR assay measure lysosomal function. The cells were exposed for 24 hrs with concentrations of EnnB in the range of 0,05 μM to 100 μM. Interestingly the lowest value of AB obtain is approximately 50% of control, while NR is going down to 0%. Thus, although not directly comparable these values were used to find the LC_{50} value of EnnB in both assays; which were calculated to be ~2,6 μM for AB and ~4,7 μM for NR, respectively. These values were used to find the relevant concentration range for the following experiments. In order to further characterize cell death, we next exposed cells in ordinary culture dishes for various concentrations of EnnB for 24 hrs, and scraped the loosely attached cells with a rubber policeman as suggested done by supplier. The cells were thereafter stainined with Propidium Iodide (PI) and Hoechst 33342 and analysed by fluorescence microscopy. As can be seen in figure **3B**, a concentration dependent increase in apoptotic/early apoptotic cells were obtained at the concentration of approximately 2,5 μM EnnB, reaching a maximum level of approximately 15%. A very high level of necrotic cells (~50%) was obtained for DMSO treated; and no clear concentration dependent increase due to EnnB could be observed.

To check whether the level of necrotic cells could be an artefact due to the scraping of cells for microscopic preparation, we next tried out some UpCell™ dishes (used as described in materials and methods). By placing these dishes on ice, the cells were easily detached without damaging the plasma membrane. In the following preparation of the samples, the number of necrotic cells in the control was reduced to approximately 3%, which would be as expected (**fig. 3C**). Based on microscopy observations of dyed cells, the cells were divided into groups of necrotic, apoptotic, and early apoptotic (apo*). Typically, the early apoptotic cells have some morphological characteristics of apoptotic cells. Instead of having fully condensed nuclei, they have rather a donut-like chromatin condensation. The total number of cells with apoptotic morphological features was observed to be significant in cells exposed of 5 μM and 10 μM EnnB and was 6% and 11% respectively, compared to 1% observed in control. Also the number of necrotic cells

were increased following exposure with Enn , from 3% in the control up to 7% in cells exposed to 10 μM Enn B.

A similar trend was observed while analyzing apoptosis by flow cytometry after 24 hr exposure to EnnB. In this assay apoptotic cells with condensed chromatin would be less stained with PI than viable cells and thus appear as a Sub-G_1 peak in an analysis by flow cytometer. A 10-20% increase in the sub-G_1 population was measured in cells exposed with EnnB compared to the control, with the higher percentage in cells exposed of 5 and 10 μM (**fig. 3D**).

The annexin V assay was used to further characterize cell death. Together with PI staining the difference in phosphatidyl serine (PS) distribution was used to divide the cells into viable (not shown), (early) apoptotic, and late apoptotic or necrotic cells (**fig. 4A and 4B**). This analysis revealed an increase in the number of apoptotic cells after 24 hrs of exposure, and was measured to 20% in the cells exposed with 10 μM EnnB, compared to 5% apoptotic cells in the control. There is no significant increase in the number of cells with late apoptotic or necrotic features, and neither in the level of cleaved caspase 3 in cells exposed for 24 hrs. To measure secondary DNA damage due to DNA fragmentation during the apoptotic process, we used the TUNEL analysis, a method often used to detect apoptotic cells (**fig. 4D and 4E**). In cells exposed for 24 hrs there is a minor increase in levels of detected dUTP, compared to the control .TUNEL positive cells were increased to 6% after exposure to 2,5 μM EnnB, while only 2% could be seen in controls receiving DMSO only**.**

Effects on cell cycle

The effects on the cell cycle were analyzed after both 8 and 24 hr exposures (**fig. 5A and 5B**). In contrast to the control, cells exposed of EnnB for 24 hrs show an arrest in the G_1-phase of the cell cycle when exposed of 1,25 μM EnnB or higher concentrations. In the cells exposed of EnnB, the number of cells in the G_1 phase was increased to 75-85% compared to approximately 50% found in the control. In cells exposed for 8 and 4 hrs (4 hrs not shown) no significant increase in G_1 could be observed.

To further characterize these alterations in the cell cycle progression the protein levels of the cell cycle associated proteins, cyclin D1 and cyclin E, were measured with Western blotting in cells

exposed of EnnB for 24 hrs. The blots revealed a marked down-regulation of cyclin D1, while cyclin E was up-regulated (**fig. 6A and 6B**). EnnB also slightly up-regulated the levels of p27 Kip1 (**6C**).

Changes in morphology

During regular microscopy observations of cells after exposure it seemed to be a difference between cells exposed of EnnB and DMSO (**fig. 7A**). This observation was further investigated by counting cells with a stretched, elongated morphology in cells exposed of 10 μM EnnB and control cultures (**fig. 7B**). A difference was observed already at 4 hrs, and after 24 hrs 15% elongeated cells was observed after EnnB exposure versus 5% in cells exposed of DMSO.

As this type of morphology has been suggested to be caused by a differentiation to M2 macrophages, often characterized by increased levels of the CD163 transmembrane protein. Thus, the expression of CD163 in RAW cells exposed to EnnB for either 6 or 24 hrs was analyzed both with flow cytometry and fluorescence microscopy, (**fig. 7C and 7D**). Compared to the control the cells exposed of 10 μM EnnB showed no difference in the expression of CD163 using either of the two methods. However, cells with the characteristic elongated morphology were also observed in the samples fixed for fluorescence microscope.

DNA damage and DNA damage response (DDR)

Single cell electrophoresis (comet assay) was used to measure DNA damage, detecting single-stranded DNA breaks (SSB) and/or alkali labile sites measured as an increase in the percentage of DNA in the tail (comets). Cells exposed of 2,5 μM and 5 μM EnnB for 24 hrs showed no increase in DNA damage compared to the DMSO control (**fig. 8B**). Furthermore, no increase in tail moment was seen after addition of fpg, an enzyme that converts 8-oxo-7,8-dihydro-2'-guanosine (8-oxodGuo) to SSB.

To measure any possible DNA damage not detected by the comet assay, we measured the levels of some central proteins involved in the DNA damage response by Western blotting and flow cytometry. However, cells exposed to EnnB (2,5 , 5 and 25 μM) for 24 hrs, showed no marked

changes in the levels of p-p53 (Ser 15 and Ser 392) and p21 measured by either of the two methods, when compared to controls, as can be seen in figures **8C-8F.** Analysis of γH2A.X was performed with flow cytometry only, and a slight up-regulation of the phosphorylated form of H2A.X was observed in cells exposed of 5 μM EnnB for 24 hrs (**fig 8G**).

Effect on Endocytosis

The organization of membrane microdomains were studied by use of fluorescence microscope. A difference in this organization was observed when exposed cells were fixed promptly after incubation with FITC coupled CTX subunit B (Ctx B) (**fig. 9A**), compared to the cells fixed after incubation with FITC coupled Ctx B for 2 hrs (**fig. 9B**). Prior to fixation the cells were exposed with EnnB (10 μM) or DMSO for 24, and the cells exposed of EnnB show an inhibition in the internalization of the Ctx B in contrast to the control (**fig. 9B**)

Lysosomal damages

To investigate the possible involvement of lysosomes in the EnnB induced effects on exposed cells, micrographs of these and DMSO exposed cells were prepared. (**fig. 10A and 10B**) After 24 hr exposure these revealed some accumulation of lipids inside the lysosomes (**fig. 10B**; *white arrows*), which is a sign of lysosomal dysfunction.

Activation of caspase-1

As EnnB has been suggested to act as a cation ionophore and seems to cause lysosomal damage, both known to trigger an activation of the inflammasome, the role of caspase-1 in EnnB-induced cell death was investigated with its inhibitor ZYVAD-FMK. Cells were exposed with ZYVAD-FMK (10 μM) for 30 min prior to the 24 hr long EnnB (10μM) exposure, and cell death was characterized with a fluorescence microsope (10A). The addition of the inhibitor reduced the total amount of apoptotic cells from from 5% to less than 1%. ZYVAD-FMK seems, however, to have no or little effect on the number of necrotic cells.

Further analysis of caspase-1 activation was done by Western blotting (**fig. 10B**). In cells exposed of EnnB (2,5, 5 and 10 μM) for 24 hrs a down-regulation of caspase-1 (48 kDA) and an up-regulation of its cleaved form (p20) is observed.

Cytokine response

As a next step, in order to further examine any possible activation of the inflammasome after exposure to EnnB, we pretreated the cells with LPS, which is known to cause accumulation of pro-IL-1β and measured the IL-1 β release in cells exposed to EnnB and compared with DMSO controls. First we did some preliminary experiments with various LPS / cell concentration. (**fig. 11A and 11B**). These results revealed that an LPS-concentration of 25 ng/mL in addition to seeding 500 000 cells per mL (~135 000/cm^2) gave the most optimal experimental conditions. Based on published literature [30] the cells were primed for three hrs with LPS prior to exposure with EnnB and DMSO, and the release of IL-1 β measured after 6 hrs.

This was followed by exposing both un-primed and LPS-primed cells with DMSO and different concentrations of EnnB (2,5 , 5 and 10 μM). As shown in figure **11C** the amount of IL-1β released from LPS-primed cells exposed of EnnB was all in the range of 125-190 pg/mL, compared to (>20 pg/mL) in the cells exposed of DMSO, and as expected, even lower (>10 pg/mL) in the un-primed cells.

Pro-IL-1β is cleaved to its active form (IL-1β) by caspase-1. The effect of caspase-1 was demonstrated by treatment with ZYVAD-FMK prior to EnnB (10 μM) exposure in cells already primed with LPS. The results is shown in figure **11D**, where a significant difference is observed in the amount of IL-1β released from cells with inhibition of caspase-1. In addition to exposure with EnnB cells primed with LPS were also exposed of 100 nm silica particles (500 μg/mL) and MinUsil (500 μg/mL). These particles were used as positive controls and gave a release of cytokines in similar amounts of EnnB (data not shown).

Activation of NF-κB

Activation of NF-κB can lead to accumulation of pro-IL-1β. In figure **13A**, cells exposed with 5 μM of EnnB for 24 hrs show an up-regulation in the levels of NF-κB, compared to the control. IκBα is a cytosolic inhibitor of NF-κB and is phosphorylated and degraded in response to activation. (**fig. 13B and 13C**) A down-regualtion of IκBα was observed with Western blotting in cells exposed of EnnB (1,25, 2,5 and 5μM), compared to the control. The cells analyzed in figure **13B** were primed for 3 hrs with LPS followed by exposure to EnnB or DMSO. The results presented in figure **13C** come from cells exposed for either EnnB or DMSO for 24 hrs.

Supplementary results

As for the RAW 264.7 the release of IL-1β was measured in J774A.1 cells, in order to examine activation of the inflammasome.The secretion of IL-1β in the collected supernatant of exposed cells was analyzed using ELISA. In the preliminary experiments done with the J774A.1 cells we found that pre-treatment for three hrs a LPS concentration of 25 ng/mL accompanied with seeding 600 000 cells/ml (160 000/cm^2) gave the most optimal experimental conditions (**sup. fig. IV and V**). In the following experiments primed and un-primed J774A.1 cells were exposed with different concentrations of EnnB (2,5 , 5 and 10 μM) or DMSO for 6 hrs. As expected, the results showed that cells without pre-treatment secreted IL-1β in minor amounts (>10 pg/mL) , and in the pre-treated cells a significant enhancement in the release was observed in cells exposed of EnnB (**sup. fig. VI**). The release in the primed cells was measured to approximately 140, 100, and 90 pg/mL in the cells exposed of 2,5 , 5 and 10 μM EnnB, respectively.

Further, we analysed the effect on IL-1β release in primed J774A.1 cells treated with ZYVAD-FMK (caspase-1 inhibitor) prior to exposure with EnnB (10 μM) (6 hrs). Again a significant difference in the amount of IL-1β secreted was observed in cells treated without and with the inhibitor of caspase-1 (**sup. fig.VII**).

Hence, the release of IL-1B in LPS-primed cells indicates that EnnB is able to activate the inflammasome mediated inflammatory response in both RAW 264.7 and J774A.1 cells.

The J774A.1 cells were also arrested in the G1- phase of the cell cycle (**sup. fig. I**). In cells exposed with EnnB (1,25 , 5 and 10 μM) or DMSO, approximately 88% of the cells where analysed to be in G_1, already in response to 1,25 μM of EnnB.

In contrast to the results found concerning expression of CD163 in the RAW 264.7 cells, we found an increase in expression of the transmembrane protein in the J774A.1 cells after exposure with EnnB. In the analysis done with flow cytometry the cells were exposed with either EnnB (5 μM) or DMSO for 24 hrs, as shown in supplementary figure **II** an increase in CD163 expression is observed. A similar result was found when exposing cells for 6 hrs with either EnnB (10 μM) or DMSO followed by fluorescence microscopy observations **(sup. fig. III)**.

Discussion

It is hypothesized that the cytotoxic effect of enniatins are caused by its ability to function as an ionophore, forming channels in cellular lipid membranes [6,7]. Here we report that EnnB reduce proliferation by a G_1-arrest in RAW 264.7 cells, and induced some caspase-1 dependendent apoptosis. No or little primary DNA–damage/DNA-damage response was observed. The most noteworthy finding was that EnnB exposure in combination with lipopolysaccharide (LPS) resulted in inflammasome activation, possibly the NLRP3 inflammasome, followed by secretion of IL-1β.

The toxicity tests alamar blue (AB) and neutral red (NR) are simple to perform and may give information regarding effects on cell proliferation as well as mechanisms involved. In the AB assay (**fig. 2A**) functional mitochondria are needed to reduce the substrate giving off fluorescence, and the measured fluorescence is proportional to the number of viable cells [25] The IC_{50} value of EnnB in this assay was calculated to 2,6 μM. Interestingly, the measured signal stabilized in the range of 50-40%, compared to the control, for concentrations up to 100 μM. This reduction in fluorescence intensity might be a result of a G_1-cell cycle arrest (**fig. 5B**) rather than any primary mitochondrial damage, as fewer cells by it self will reduce the fluorescence signalling. In contrast when using the NR assay (**fig. 2B**), measuring the membrane permeability of lysosomes, a more pronounced effect was observed after EnnB exposure. At the highest concentrations, the NR-values were reduced to values close to zero suggesting that the lysosomes were highly damaged. Thus, these experiments suggest that the lysosomes may be an important primary site of EnnB toxicity. In the NR assay the IC_{50} of EnnB was calculated to 3,4 μM. In a study by Ivanova *et al.* [3] with MRC-5 cells, the IC_{50} of EnnB was in the range of 1,9-to 6,9 μM. By using the MTT cell viability assay, another study has shown IC_{50} values for a mixture of enniatins to be in the range from 7,9 to >10 μM [11]. In a study on the mitochondrial effects of mixtures of enniatin and EnnB alone, the enniatin mixture was shown to be more damaging to the mitochandria than EnnB [8]. Thus, the cytotoxicity of EnnB observed with AB and NR assays was well agreement with previous studies.

Microscopic examinations of cell stained with PI and Hoechst revealed that EnnB induced morphological features associated with apoptosis and necrosis (**fig. 3A**). EnnB induced cells with a reduced cellular volume, condensed and fragmented nuclei, defined as apoptotic, and PI

positive cells with increased cellular volume as necrotic. Some cells with morphological characteristics similar to the apoptotic but with a ring shaped chromatin condensation were defined as early apoptotic (apo*). This type of apoptosis could be the result of incomplete DNA-fragmentation and may involve other proteases than the classic apoptotic caspases [31]. In our first sets of experiments very high numbers of necrotic cells were counted both in the controls and in the exposed cells (**fig. 3B**). As control cells in the culture dish seemed viable when examined by light microscopy, we anticipated that this could be due to an artefact. More specifically that we induced membrane effect when preparing the cells for nuclear staining, as the procedure suggested that the cells should collected by scraping with a rubber policeman. Indeed, by modifying this procedure by using the UpCell dishes it which cells automatically detached when placed on ice (**fig. 3C**), the percentage of necrotic cells where reduced from 50% to 3% and from 56% to 6% for DMSO and EnnB (10 μM), respectively. After the EnnB exposure around 12% of the cells showed morphological features of apoptosis.

There are several morphological and biochemical methods that can be used to characterize apoptosis. In this study we have also determined apoptosis by analysis of the sub-G_1 peak, annexin V staining after externalization of phosphatidylserine (PS), the activation of caspase-3 with specific antibodies and quantification of TUNEL-stained cells by flow cytometric analysis. In combination with the cell cycle analysis, we observed a sub-G_1 peak. This smaller peak in the cell cycle profile is caused by less PI staining of the DNA, due to chromatin condensation and nuclear fragmentation. The sub-G_1 signal is detected when the DNA dye is incorporated to apoptotic bodies, smaller than the viable cells observed in the cell cycle profile. EnnB is clearly giving such an effect (**fig. 3D**), but an accurate quantification of the chromatin condensation can not be measured by this method as more than one apoptotic body could have originated from a single viable cell. In viable cells the distribution of PS is asymmetric, with PS found in the inner leaflet of the plasma membrane. Exposure of PS on the surface of apoptotic cells seems to be one of the most important ("eat-me") signals for recognition by neighbouring macrophages [32]. Using the annexin V assay this biochemical feature of apoptosis could be investigated (**fig. 4A**), and the cells could be divided into early apoptotic or late apoptotic/necrotic cells. Again EnnB induced an increase in the number of (early) apoptotic cells, while the number of necrotic cells were unaffected, compared to the control. Interestingly, translocation of PS to the outer leaflet of the plasma membrane is also described as an early marker of caspase-3 activation during apoptosis [33]. Therefore, we also measured the intracellular levels of cleaved caspase-3, which was observed to be somewhat increased after EnnB exposure (**fig. 4C**). The TUNEL assay is a

method for detecting apoptotic cells that exhibit DNA fragmentation. Cleavage of caspase-3 is often found to be central in the apoptotic process and mediate the activation of DNA endonucleases resulting in DNA fragmentation [34]. The DNA fragmentation observed with the TUNEL assay is a result of the apoptotic signalling cascade, and may be referred to as a secondary DNA damage. We have observed condensed nuclei and apoptotic bodies as an effect of EnnB in examinations with microscopy and in determination of the sub-G_1 peak. We have also seen flipping of PS and some fragmentation caused by the apoptotic cascade, both as a result of activated caspase-3. In addition to the presented results, it would be of future interest to use these assays to follow the apoptotic process induced by EnnB over time

The cell death analysis have shown that EnnB induce apoptosis in approximately 6-20% of the cells, depending on the assay used. The induced apoptosis seems to be independent of the much more significant cell cycle arrest (described below), The cell cycle arrest in G_1 was found in cells exposed with EnnB for 24 hrs (**fig. 5B and supp. fig. I**) is in accordance with the restrained proliferation suggested by the AB assay and by visual examinations of exposed cells (**fig. 7A**). Progression in the cell cycle is regulated by cyclins and cyclin dependent kinases (CDK), and cyclin-CDK complexes are in turn regulated by cyclin-dependent kinase inhibitors (CDKI), which generally inhibit cell cycle progression [35]. The progression from G_1 to S, in the cell cycle, is regulated by cyclin D (1,2,3) and cyclin E, with their respective partners CDK4/6 and CDK2. Normally, in the progression of the cell cycle, pairing of the D-type cyclins with their catalytic partners CDK4 and CDK6 happens early in G_1 and inactivates CDKIs, like p27 (Kip1) (p27), a CDKI from the Cip/Kip family [36]. The cyclin D-CDK complex will in addition activate the transcription factor E2F by phosphorylation of retinoblastoma (Rb), resulting in an increase of cyclin E and cyclin A (cyclin A is a S-phase cyclin). In the EnnB exposed cells the levels of cyclin D1 were reduced, while the protein levels of p27 were increased (**fig. 6A and 6C**). The western analysis of cells exposed with EnnB also revealed an up-regulation in the levels of cyclin E. Since p27 is working downstream of cyclin D1, diminished levels of cyclin D1 and an increase in the p27 levels seems to fit with the current model of transition from G_1 to the S-phase of the cell cycle [36]. At first, we would also expect a down-regulation in the cyclin E levels, but since we are looking at a “snap-shot” of the protein levels after 24 hrs of EnnB exposure it is not possible to predict whether the levels are on the rise or on the fall. EnnB might cause an arrest late in the G_1-phase. Further research is needed to fully understand the background of the G_1-arrest, and the levels of cyclins, CDKs and their inhibitors should be

analysed and followed over time. In a study of a mixture of enniatins [11], the levels of cyclin D1 was also reported to decrease.

An inhibition of cell proliferation is often associated with a differentiation process. In a previous study, we found that expure to chemicals (phthalates) may induce morphological differentiation of macrophages [34]. Thus, we closer analyzed the morphology of EnnB-exposed cells with light microscopy and observed that some of the Raw 264.7 cells displayed an elongated morphology suggestion some kind of differentiation (**fig. 7A and 7B**). Interestingly, another mycotoxin Alternariol (AOH) is found to cause differentiation of RAW 264.7 cells into round cells with tentacle like elongations, suggested to be dendritic-like cells (Solhaug *et al.* – manuscript in preparation). Activated macrophages have been shown to be polarized in response to different inducers, thereby acquiring different functional properties. The macrophages have been suggested to be classified into M1 and M2 (2a, 2b, 2c) based on inducer and the following response [27]. Often M1 is associated with dendritic like cell morphology and pro-inflammatory properties, whereas anti-inflammatory M2 cells often are found to be of the elongated type, as those seen after EnnB exposure [37]. CD163 is a transmembrane protein found to be expressed on M2-like macrophages, which is generally involved in immuno-regulation, killing of parasites, and tissue remodelling [27]. According to the results (**fig. 7C and 7D**), there is no difference in the levels of CD163 found in the EnnB exposed cells, versus the controls. However, in experiments done with our second cell line, the J774A.1 mouse macrophages, EnnB caused an up regulation of CD163 (**sup.fig. II and III**). To further investigate this interesting issue of potential macrophage differentiation, other markers of M1 and M2 should be used in addition to CD163.

In response to DNA-damage a cell might be arrested in the cell cycle, giving time for promotion of the DNA repair machinery. An activation of p53, "the guardian of genome", often results in an arrest in the G_1/S transition phase [38]. Thus, we used the comet assay to find out if EnnB caused any primary DNA damage. The Comet assay detects alkali labile sites, single and double stranded DNA breaks, and DNA unwinding as a result of DNA repair. The tail (comet) intensity is measured as a parameter for the DNA damage. In accordance with other studies [11, 39], we found no difference in the intensity measured in cells exposed of EnnB, compared to the control (**fig. 8B**). Phosphorylation of p53 is connected to cell cycle arrest and apoptosis [40], and activated p53 promotes transcription of, among others, the tumor suppressor protein p21 (Waf1/Cip1) (p21) which is associated with G_1-arrest in the cell cycle [41]. Histone H2A.X, a member of the H2A family, is also involved in checkpoint mediated cell cycle arrest and DNA

repair following dsDNA breaks, which is a highly lethal DNA damage [42]. Phosphorylated H2A.X (γH2A.X) is also formed as a consequence of DNA fragmentation during apoptosis [43]. Based on the results showing a G_1-arrest and some fragmentation of DNA after exposure to EnnB, the protein levels of p-p53, p21 and γH2A.X were analysed by flow cytometry and/or Western blotting after 24 hrs exposure. The data on p-p53 (**fig. 8C and 8E**) and the unchanged levels of p21 after exposure to EnnB (**fig. 8D and 8F**), suggests none or a minimal effect on the activation of p53, while. This is well in agreement with the study on mixtures of enniatins [11], concluding that the cytotoxic effects of enniatins are mediated by a p53 independent mechanism. Interestingly, the levels of γH2A.X was unregulated (**fig. 8G**), which support the (slight) increase in cells with DNA fragmentations found in the TUNEL analysis (**fig. 4D and 4E**). In contrast to a rapid phosphorylation of H2A.X caused by primary induced double stranded DNA-breaks, reported in response to the mycotoxin satratoxin G [34], an increase in γH2A.X after 24 hrs in combination with increased TUNNEL, suggest DNA fragmentation caused by the apoptotic process.

The NR assay (**fig. 2B**), and the ionophoric properties of EnnB [6,7] suggested that the cellular plasma membranes and lysosome activity could be affected. In a study by Tekpli *et al.* [44] plasma membrane remodelling, more specifically disruption of membrane rafts, were found to be an important early apoptotic effect. Membrane rafts are plasma membrane microdomains containing cholesterol, spingolipids and saturated acyl chains, and have been reported to be implicated in cell death [45]. In the present study we show that EnnB had no effect on the integrity of the plasma membrane rafts as marked with cholera toxin subunit B (Ctx B) (**fig. 9A**) . However, we found that EnnB inhibited the endocytosis/membrane recycling process of receptors, as the endocytotic processes of Ctx B were markedly inhibited (**fig. 9B**). Furthermore, electron microscopic examination of cells exposed to EnnB showed damages to the lysosomes as phospholipidosis, or lipid accumulation [46], which is a sign of lysosomal damage was observed (**fig. 10B**). The effect of EnnB on lysosomes, as discussed earlier, together with EnnB working as K^+ ionophore led us to the hypothesis that EnnB could trigger an activation of caspase-1 through these mechanisms. The NLRP3 inflammasome is reported to be activated by a K^+ efflux, triggered by pore-forming bacterial toxins [47]. Furthermore, in a recent paper by Kankkunen and coworkes [48] the mycotoxins, satratoxins and T-2 toxin were shown to activate caspase-1 in an inflammatory response involving the NLRP3 inflammasome in (human) macrophages

Inflammasomes, such as NLRP3, are multi protein complexes that mediate caspase-1 dependent processing of cytokines such as IL-1β [49]. To investigate the possible involvement of caspase-1 in the EnnB-induced apoptotic process, cells treated with an inhibitor of caspase-1 (ZYVAD-FMK) and examined in microscopy after nuclear staining. By inhibition of caspase-1 the percentage of cells with apoptotic features were significantly decreased (**fig. 11A**). Caspase-1 is synthesized as an inactive zymogen and controlled by proteolytic activation, i.e. by reduced intracellular K^+ or and intracellular acidification / leakage of cathepsin-B from damaged lysosomes [50]. Furthermore, analysis done by Western blotting indeed revealed a decrease in the levels of pro-caspase-1 and an increase in cleaved caspase-1 (p20) after exposure to EnnB (**fig. 11B**), suggesting that these could be likely explanations. A similar activation of caspase 1 has been reported in response to trichothecenes [48]. Interestingly, ZYVAD-FMK did not inhibit EnnB-induced necrosis, showing that the necrotic cell death is independent of caspase-1 activation and are probably related to direct membrane damage.

NALP3 belongs to a class of NOD-like receptors (NLRs), which are a type of intracellular pattern recognition receptors (PRR), and are one of several proteins found in the inflammasomes. The NLR recognize pathogen-associated molecular patterns (PAMPs) and host-derived danger signals (danger-associated molecular patterns, DAMPs) [51]. Ionophoric properties, and NR assay indicated lysosomal activity, the micrographs of EnnB exposed cells showing EnnB affecting the lysosomes of the cell verified this suggestion (**fig. 10B**). Damages in the lysosomes have been proposed as a mechanism activating the inflammasomes, where the inflammasome recognize components of lysosomes as endogenous danger signals, or DAMPs [52]. In another model the inflammasome is activated by K^+ efflux, as shown by a stimulation of the ATP-gated P2X7R by extra-cellular ATP; A limited efflux seems to triggering IL-1β release, whereas larger efflux triggering the apoptotic process [53].

To further clarify any possible inflammasome activation we measured secretion of mature IL-1β as a marker of activation. Priming with LPS causes activation of NF-κB in response to stimuli of the membrane bound toll-like receptor 4 (TLR4), and results in accumulation of intracellular pro-IL-1β [52]. Most interestingly, the LPS-primed cells had a marked increased in secretion of IL-1β after exposure with EnnB (**fig. 12A-12C**) when compared with the various controls. Furthermore, the LPS/EnnB-induced IL-1β release could be considerably reduced by the caspase-1 inhibitor (**fig. 12D**), strongly suggesting that an activation of caspase-1 is involved in the process. The mechanisms for inflammasome activation described above, all concerns activation of the NLRP3

inflammasome (also called NALP3 or cryoporin). The NLRP3 inflammasome consists of the PRR NLRP3, apoptotic speck protein containing a C-terminal caspase recruitment domain (ASC), and caspase-1. There have been reports concluding that RAW 264.7 cells lack the adaptor protein ASC, and should not be able to process and release mature IL-1β [54]. Our results show an activation of caspase-1 and secretion of IL-1β, but we can not say for certain whether this is caused by activation of the NALP3 inflammasome. Other inflammasomes, like NLRP1 and IPAF, are also able to active caspase-1 [51]. On the other hand, data from Sandberg *et al.* (manuscript in preparation) have shown activation of the NALP3 inflammasome in RAW 264.7 cells by exposure to non-crystalline silica nonoparticles, as a reduced IL-1β released were observed in cells with reduced NALP3 using specific siRNA. An important issue to consider is that the effect seemed to be highly dependent on cell concentration needed for proper measurements of IL-1β secretion. This could indicate that EnnB causes a primary effect on the cells, and when the cells are grown close enough secreted cytokines or other signal molecules (DAMPs) cause an activation of the inflammasome – as a secondary effect. However, another explanation could be the limited sensitivity of the assay used for IL-1β detection. Both explanations should be further clarified, possibly by using another method for detection of cytokines (i.e. Bio-Plex). We have also shown similar effects of LPS/EnnB on secretion of IL-1β in J774A.1 cells (**sup. fig IV-VII**), with reported ASC activity [54].

NF-κB is a transcription factor held in the cytosol in an inactive state by the inhibitory IκB proteins. Activation of NF-κB is mediated through a phosphorylation of IκBα followed by proteasome-mediated degradation of the inhibitor. The result is translocation of active NF-κB. NF-κB is activated by a highly diverse group of extracellular signals including inflammatory cytokines, growth factors, and chemokines. [55]. Both NF-κB and mitogen activated protein (MAP) have been implicated in regulation of pro-IL-1β transcription. [56,57]. We have shown increased levels of NF-κB after 24 hr exposure to EnnB (**fig. 13A**), and a downregulation of the inhibitory IκBα (**fig. 13B and 13 C**). The effect on the inhibitor, IκBα, was seen after 24 hrs exposure to EnnB and after priming with LPS followed by 6 hrs EnnB exposure. Thus, an activation of NF-κB seems to be implicated in the LPS/EnnB-induced IL-1β release; whereas the activation observed after EnnB exposure for 24 hr would suggest that EnnB by itself can result in the triggering of cytokines/chemokines. This possibility should be further explored. However, it is interestingly to note that some other enniatins have been reported to moderately inhibit tumor necrosis factor alpha (TNF-alpha)-induced NF-kappaB activation [12]; thus having an anti-

inflammatory response more in accordance with our observation of apparent M2-cell like differentiation.

In conclusion, EnnB cause a G_1-cell cycle arrest, morphological features related to apoptosis, and inflammasome activation in combination with LPS. An overall evaluation of results suggests that the apoptotic effect in cells exposed of EnnB seems to be triggered by activation of the inflammasome. The results show activation of IL-1β and caspase-1. EnnB show a synergic effect with LPS in cells primed prior to exposure and may potentially activate the inflammasome by working as a K^+-ionophore in the plasma membrane, or by causing damage to the lysosomes. The implicated synergic effect of EnnB in combination with LPS is of concern in relation to undesirable inflammatory response. More complex test systems would be of interest for future studies.

Acknowledgements

The work was funded by Norwegian Research Council through the project *Toxicological characterization of selected secondary fungal metabolites in Norwegian grain*.

References

1. Jestoi, M., *Emerging Fusarium-Mycotoxins Fusaproliferin, Beauvericin, Enniatins, And Moniliformin—A Review.* Critical Reviews in Food Science and Nutrition, 2008. **48**(1): p. 21 - 49.
2. Jestoi, M., M. Rokka, and K. Peltonen, *An integrated sample preparation to determine coccidiostats and emerging Fusarium-mycotoxins in various poultry tissues with LC-MS/MS.* Molecular Nutrition & Food Research, 2007. **51**(5): p. 625-637.
3. Ivanova, L., E. Skjerve, G.S. Eriksen, and S. Uhlig, *Cytotoxicity of enniatins A, A1, B, B1, B2 and B3 from Fusarium avenaceum.* Toxicon, 2006. **47**(8): p. 868-876.
4. Jestoi, M., M. Rokka, T. Yli-Mattila, P. Parikka, A. Rizzo, and K. Peltonen, *Presence and concentrations of the Fusarium-related mycotoxins beauvericin, enniatins and moniliformin in finnish grain samples.* Food Additives and Contaminants, 2004. **21**(8): p. 794 - 802.
5. Uhlig, S., M. Jestoi, and P. Parikka, *Fusarium avenaceum -- The North European situation.* International Journal of Food Microbiology, 2007. **119**(1-2): p. 17-24.
6. Ovchinnikov, Y.A., V.T. Ivanov, A.V. Evstratov, I.I. Mikhaleva, V.F. Bystrov, S.L. Portnova, T.A. Balashova, E.N. Meshcheryakova, and V.M. Tulchinsky, *The enniatin ionophores. Conformation and ion binding properties.* International Journal of Peptides and Protein research, 1974. **6**: p. 465-498.
7. Kamyar, M., P. Rawnduzi, C.R. Studenik, K. Kouri, and R. Lemmens-Gruber, *Investigation of the electrophysiological properties of enniatins.* Archives of Biochemistry and Biophysics, 2004. **429**(2): p. 215-223.
8. Tonshin, A.A., V.V. Teplova, M.A. Andersson, and M.S. Salkinoja-Salonen, *The Fusarium mycotoxins enniatins and beauvericin cause mitochondrial dysfunction by affecting the mitochondrial volume regulation, oxidative phosphorylation and ion homeostasis.* Toxicology, 2010. **276**(1): p. 49-57.
9. Tomoda, H., X.H. Huang, J. Cao, H. Nishida, R. Nagao, S. Okuda, H. Tanaka, S. Omura, H. Arai, and K. Inoue, *Inhibition of acyl-CoA: cholesterol acyltransferase activity by cyclodepsipeptide antibiotics.* The Journal of Antibiotics, 1992. **45**: p. 1626-1632.
10. Trenin, A.S., I.V. Tolstykh, L.P. Terekhova, V.A. Zenkova, M.O. Makarova, E.G. Gladkikh, O.P. Bychkova, G.S. Katrujha, and I.V. Dudnik, *The hypolipidemic action of*

antibiotic 86/88 (enniatin B) in a hepatoblastoma G2 cell culture. Antibiot Khimioter., 2000. **45**: p. 6-9.

11. Dornetshuber, R., P. Heffeter, M.-R. Kamyar, T. Peterbauer, W. Berger, and R. Lemmens-Gruber, *Enniatin Exerts p53-Dependent Cytostatic and p53-Independent Cytotoxic Activities against Human Cancer Cells.* Chemical Research in Toxicology, 2007. **20**(3): p. 465-473.
12. Wätjen, W., A. Debbab, A. Hohlfeld, Y. Chovolou, A. Kampkötter, R.A. Edrada, R. Ebel, A. Hakiki, M. Mosaddak, F. Totzke, M.H.G. Kubbutat, and P. Proksch, *Enniatins A1, B and B1 from an endophytic strain of Fusarium tricinctum induce apoptotic cell death in H4IIE hepatoma cells accompanied by inhibition of ERK phosphorylation.* Molecular Nutrition & Food Research, 2009. **53**(4): p. 431-440.
13. Hiraga, K., S. Yamamoto, H. Fukuda, N. Hamanaka, and K. Oda, *Enniatin has a new function as an inhibitor of Pdr5p, one of the ABC transporters in Saccharomyces cerevisiae.* Biochemical and Biophysical Research Communications, 2005. **328**(4): p. 1119-1125.
14. Dornetshuber, R., P. Heffeter, M. Sulyok, R. Schumacher, P. Chiba, S. Kopp, G. Koellensperger, M. Micksche, R. Lemmens-Gruber, and W. Berger, *Interactions between ABC-transport proteins and the secondary Fusarium metabolites enniatin and beauvericin.* Molecular Nutrition & Food Research, 2009. **53**(7): p. 904-920.
15. Ivanova, L., S. Uhlig, G. Eriksen, and L. Johannessen, *Enniatin B1 is a substrate of intestinal P-glycoprotein, multidrug resistance-associated protein 2 and breast cancer resistance protein.* World Mycotoxin Journal, 2010. **3**(3): p. 271-281.
16. Gäumann, E., S. Naef-Roth, and L. Ettlinger, *Zur gewinnung von enniatinen aus dem myzel verschiedener Fusarien.* Phytopath. Z, 1950. **16**: p. 289-299.
17. Bosch, U., C.J. Mirocha, H.K. Abbas, and M. di Menna, *Toxicity and toxin production by Fusarium isolates from New Zealand.* Mycopathologia, 1989. **108**: p. 73-79.
18. McKee, T.C., H.R. Bokesch, J.L. McCormick, M.A. Rashid, D. Spielvogel, K.R. Gustafson, M.M. Alavanja, J.H. Cardellina, and M.R. Boyd, *Isolation and Characterization of New Anti-HIV and Cytotoxic Leads from Plants, Marine, and Microbial Organisms1.* Journal of Natural Products, 1997. **60**(5): p. 431-438.
19. Takeda, K. and S. Akira, *Toll-like receptors in innate immunity.* International Immunology, 2005. **17**(1): p. 1-14.
20. Raetz, C.R.H. and C. Whitfield, *Lipopolysaccharide endotoxins.* Annual Review of Biochemistry, 2002. **71**(1): p. 635-700.

21. Tai, J.H. and J.J. Pestka, *Synergistic interaction between the trichothecene T-2 toxin and Salmonella typhimurium lipopolysaccharide in C3H/HeN and C3H/HeJ mice.* Toxicology Letters, 1988. **44**(1-2): p. 191-200.
22. Islam, Z. and J.J. Pestka, *Role of IL-1β in Endotoxin Potentiation of Deoxynivalenol-Induced Corticosterone Response and Leukocyte Apoptosis in Mice.* Toxicological Sciences, 2003. **74**(1): p. 93-102.
23. Meca, G., J.M. Soriano, A. Gaspari, A. Ritieni, A. Moretti, and J. Mañes, *Antifungal effects of the bioactive compounds enniatins A, A1, B, B1.* Toxicon, 2010. **56**(3): p. 480-485.
24. Eldadah, B.A., A.G. Yakovlev, and A.I. Faden, *The Role of CED-3-Related Cysteine Proteases in Apoptosis of Cerebellar Granule Cells.* The Journal of Neuroscience, 1997. **17**(16): p. 6105-6113.
25. Springer, J.E., R.D. Azbill, and S.L. Carlson, *A rapid and sensitive assay for measuring mitochondrial metabolic activity in isolated neural tissue.* Brain Research Protocols, 1998. **2**(4): p. 259-263.
26. Vermes, I., C. Haanen, H. Steffens-Nakken, and C. Reutellingsperger, *A novel assay for apoptosis Flow cytometric detection of phosphatidylserine expression on early apoptotic cells using fluorescein labelled Annexin V.* Journal of Immunological Methods, 1995. **184**(1): p. 39-51.
27. Mantovani, A., A. Sica, S. Sozzani, P. Allavena, A. Vecchi, and M. Locati, *The chemokine system in diverse forms of macrophage activation and polarization.* Trends in Immunology, 2004. **25**(12): p. 677-686.
28. Azqueta, A., S. Shaposhnikov, and A.R. Collins, *DNA oxidation: Investigating its key role in environmental mutagenesis with the comet assay.* Mutation Research/Genetic Toxicology and Environmental Mutagenesis, 2009. **674**(1-2): p. 101-108.
29. Asare, N., M. Låg, D. Lagadic-Gossmann, M. Rissel, P. Schwarze, and J.A. Holme, *3-Nitrofluoranthene (3-NF) but not 3-aminofluoranthene (3-AF) elicits apoptosis as well as programmed necrosis in Hepa1c1c7 cells.* Toxicology, 2009. **255**(3): p. 140-150.
30. Pestka, J. and H.-R. Zhou, *Toll-Like Receptor Priming Sensitizes Macrophages to Proinflammatory Cytokine Gene Induction by Deoxynivalenol and Other Toxicants.* Toxicological Sciences, 2006. **92**(2): p. 445-455.
31. Leist, M. and M. Jäättelä, *Four deaths and a funeral: from caspases to alternative mechanisms.* Nat Rev Mol Cell Biol, 2001. **2**(8): p. 589-598.

32. Hanayama, R., M. Tanaka, K. Miyasaka, K. Aozasa, M. Koike, Y. Uchiyama, and S. Nagata, *Autoimmune Disease and Impaired Uptake of Apoptotic Cells in MFG-E8-Deficient Mice.* Science, 2004. **304**(5674): p. 1147-1150.
33. Martin, S.J., C.P. Reutelingsperger, A.J. McGahon, J.A. Rader, R.C. van Schie, D.M. LaFace, and D.R. Green, *Early redistribution of plasma membrane phosphatidylserine is a general feature of apoptosis regardless of the initiating stimulus: inhibition by overexpression of Bcl-2 and Abl.* The Journal of Experimental Medicine, 1995. **182**(November): p. 1545-1556.
34. Rakkestad, K.E., I. Skaar, V.E. Ansteinsson, A. Solhaug, J.A. Holme, J.J. Pestka, J.T. Samuelsen, H.J. Dahlman, J.K. Hongslo, and R. Becher, *DNA Damage and DNA Damage Responses in THP-1 Monocytes after Exposure to Spores of either Stachybotrys chartarum or Aspergillus versicolor or to T-2 toxin.* Toxicological Sciences, 2010. **115**(1): p. 140-155.
35. Lloyd, R.V., L.A. Erickson, L. Jin, E. Kulig, X. Qian, J.C. Cheville, and B.W. Scheithauer, *p27kip1: A Multifunctional Cyclin-Dependent Kinase Inhibitor with Prognostic Significance in Human Cancers.* The American Journal of Pathology, 1999. **154**(2): p. 313-323.
36. Sherr, C.J. and J.M. Roberts, *Living with or without cyclins and cyclin-dependent kinases.* Genes & Development, 2004. **18**(22): p. 2699-2711.
37. van der Plas, M.J.A., J.T. van Dissel, and P.H. Nibbering, *Maggot Secretions Skew Monocyte-Macrophage Differentiation Away from a Pro-Inflammatory to a Pro-Angiogenic Type.* PLoS ONE, 2009. **4**(11): p. e8071.
38. Schwartz, D. and V. Rotter, *p53-Dependent cell cycle control: response to genotoxic stress.* Seminars in Cancer Biology, 1998. **8**(5): p. 325-336.
39. Behm, C., G.H. Degen, and W. Föllmann, *The Fusarium toxin enniatin B exerts no genotoxic activity, but pronounced cytotoxicity in vitro.* Molecular Nutrition & Food Research, 2009. **53**(4): p. 423-430.
40. Orrenius, S., P. Nicotera, and B. Zhivotovsky, *Cell Death Mechanisms and Their Implications in Toxicology.* Toxicological Sciences, 2011. **119**(1): p. 3-19.
41. Pestell, R.G., C. Albanese, A.T. Reutens, J.E. Segall, R.J. Lee, and A. Arnold, *The Cyclins and Cyclin-Dependent Kinase Inhibitors in Hormonal Regulation of Proliferation and Differentiation.* Endocrine Reviews, 1999. **20**(4): p. 501-534.
42. Yuan, J., R. Adamski, and J. Chen, *Focus on histone variant H2AX: To be or not to be.* FEBS letters, 2010. **584**(17): p. 3717-3724.

43. Lu, C., F. Zhu, Y.-Y. Cho, F. Tang, T. Zykova, W.-y. Ma, A.M. Bode, and Z. Dong, *Cell Apoptosis: Requirement of H2AX in DNA Ladder Formation, but Not for the Activation of Caspase-3.* Molecular Cell, 2006. **23**(1): p. 121-132.
44. Tekpli, X., M. Rissel, L. Huc, D. Catheline, O. Sergent, V. Rioux, P. Legrand, J.A. Holme, M.-T. Dimanche-Boitrel, and D. Lagadic-Gossmann, *Membrane remodeling, an early event in benzo[[alpha]]pyrene-induced apoptosis.* Toxicology and Applied Pharmacology, 2010. **243**(1): p. 68-76.
45. Nourissat, P., M. Travert, M. Chevanne, X. Tekpli, A. Rebillard, G.L. Moigne-Müller, M. Rissel, J. Cillard, M.-T. Dimanche-Boitrel, D. Lagadic-Gossmann, and O. Sergent, *Ethanol induces oxidative stress in primary rat hepatocytes through the early involvement of lipid raft clustering.* Hepatology, 2008. **47**(1): p. 59-70.
46. Anderson, N. and J. Borlak, *Drug-induced phospholipidosis.* FEBS letters, 2006. **580**(23): p. 5533-5540.
47. Petrilli, V., S. Papin, C. Dostert, A. Mayor, F. Martinon, and J. Tschopp, *Activation of the NALP3 inflammasome is triggered by low intracellular potassium concentration.* Cell Death Differ, 2007. **14**(9): p. 1583-1589.
48. Kankkunen, P., J. Rintahaka, A. Aalto, M. Leino, M.-L. Majuri, H. Alenius, H. Wolff, and S. Matikainen, *Trichothecene Mycotoxins Activate Inflammatory Response in Human Macrophages.* The Journal of Immunology, 2009. **182**(10): p. 6418-6425.
49. Martinon, F., K. Burns, and J. Tschopp, *The Inflammasome: A Molecular Platform Triggering Activation of Inflammatory Caspases and Processing of proIL-[beta]*. Molecular Cell, 2002. **10**(2): p. 417-426.
50. Vancompernolle, K., F. Van Herreweghe, G. Pynaert, M. Van de Craen, K. De Vos, N. Totty, A. Sterling, W. Fiers, P. Vandenabeele, and J. Grooten, *Atractyloside-induced release of cathepsin B, a protease with caspase-processing activity.* FEBS letters, 1998. **438**(3): p. 150-158.
51. Schroder, K. and J. Tschopp, *The Inflammasomes.* Cell, 2010. **140**(6): p. 821-832.
52. Bryant, C. and K.A. Fitzgerald, *Molecular mechanisms involved in inflammasome activation.* Trends in Cell Biology, 2009. **19**(9): p. 455-464.
53. Lévesque, S.A., F. Kukulski, K. Enjyoji, S.C. Robson, and J. Sévigny, *NTPDase1 governs P2X7-dependent functions in murine macrophages.* European Journal of Immunology, 2010. **40**(5): p. 1473-1485.

54. Pelegrin, P. and A. Surprenant, *Pannexin-1 mediates large pore formation and interleukin-1[beta] release by the ATP-gated P2X7 receptor.* EMBO J, 2006. **25**(21): p. 5071-5082.

55. Landvik, N.E., V.M. Arlt, E. Nagy, A. Solhaug, X. Tekpli, H.H. Schmeiser, M. Refsnes, D.H. Phillips, D. Lagadic-Gossmann, and J.A. Holme, *3-Nitrobenzanthrone and 3-aminobenzanthrone induce DNA damage and cell signalling in Hepa1c1c7 cells.* Mutation Research/Fundamental and Molecular Mechanisms of Mutagenesis, 2010. **684**(1-2): p. 11-23.

56. Hiscott, J., J. Marois, J. Garoufalis, M. D'Addario, A. Roulston, I. Kwan, N. Pepin, J. Lacoste, H. Nguyen, and G. Bensi, *Characterization of a functional NF-kappa B site in the human interleukin 1 beta promoter: evidence for a positive autoregulatory loop.* Mol. Cell. Biol., 1993. **13**(10): p. 6231-6240.

57. Heitmeier, M.R., A.L. Scarim, and J.A. Corbett, *Double-stranded RNA-induced Inducible Nitric-oxide Synthase Expression and Interleukin-1 Release by Murine Macrophages Requires NF-κB Activation.* Journal of Biological Chemistry, 1998. **273**(24): p. 15301-15307.

Figure Legends

Figure 1. The chemical structure of EnnB.

Figure 2. Cell viability/density. RAW 264.7 cells were exposed to various concentrations of EnnB for 24 hrs. Relative cell viability/density (% optical density in exposed groups versus control groups) was measured by Alamar Blue (AB) (**2A**) and Neutral Red (NR) (**2B**) as described in Materials and Methods. The graphs shown are dose/response curves from three independent experiments, with means represented as dots (AB) or squares (NR).

Figure 3. Cell death determined by microscopy and flow cytometry. Raw 264.7 cells treated with different concentrations of EnnB or DMSO for 24 hrs. (**A**) Cells cultured in ordinary dishes, stained with PI/Hoechst and examined by fluorescence microscope. Representative pictures of various types of cells exposed of 10 μM of EnnB are shown. Original magnification, 60 x. (**B**) Cells from experiments done in ordinary culture dishes presented as mean ± SEM of three independent experiments. (**C**) Cells grown in UpCell™ dishes were exposed to EnnB for 24 hrs and stained with PI/Hoechst before analysis. Presented data is mean ± SEM of three independent experiments. (**D**) Cells grown in ordinary dishes and analyzed with flow cytometer. Presented data is mean of Sub-G_1 ± SEM of 4 independent experiments.

Figure 4. Characterization of cell death with annexin V, TUNEL and caspase-3. Raw 264.7 cells were treated with different concentrations of EnnB or DMSO for 24 hrs. (**A**) Cells grown in UpCell™ dishes were exposed, stained with FITC Annexin V, and analyzed with flow cytometry. Presented data is mean ± SEM of 4 independent experiments. (**B**) Dotplots from one representative experiment, with cells exposed of EnnB (10 μM) and DMSO are presented. (**C**) The results from one out of two measurements of cleaved caspase-3 by using flow cytometer are presented; DMSO (black); EnnB 5 μM (red). (**D**,**E**) Cells were exposed to EnnB (2,5 μM) and DMSO for 24 hrs and analyzed for DNA fragmentation with TUNEL assay.

Figure 5. Cell cycle analysis. Raw 264.7 were exposed to different concentrations of EnnB or DMSO (**A** = 8 hrs, **B** = 24 hrs). Attached and floating cells were stained with PI and analyzed with flow cytometer. Presented data is mean ± SEM of 4 independent experiments.

Figure 6. Characterization of changes in proteins involved in cell cycle regulation. (**A-C**). Raw 264.7 cells exposed to different concentrations of EnnB or DMSO for 24 hrs and analyzed for expression of Cyclin D1, Cyclin E, and p27 by Western blotting. A minimum of two independent experiments were done in regard of each protein, and one representative experiment is shown.

Figure 7. Effect on morphology. Raw 264.7 cells were exposed to EnnB (10 μM) or DMSO. (**A**) Pictures taken at 0 hrs and 24 hrs, original magnification, 20 x. (**B**) Cells with stretched morphology counted at 0 hrs, and after 2, 4, 6, and 24 hrs. The presented data show mean ± SEM of 300 cells counted in 5 sectors (per cell dish) after different exposure periods. (**C**) Cells grown in UpCell™ dishes, exposed of EnnB (10 μM) and DMSO for 24 hrs, stained with AF488 coupled AB for CD163, and analyzed by flow cytometry; DMSO (black), EnnB (red). (**D**) Cells exposed of EnnB (10 μM) and DMSO for 6 hrs, stained with AF488 coupled AB for CD163, and observed with fluorescence microscopy. Original magnification, 100 x.

Figure 8. DNA damage and DNA damage response (DDR). RAW 264.7 cells exposed of EnnB and DMSO for 24 hrs and analyzed by single cell gel electophoresis (alkaline comet assay) (**A and B**). (**A**) Pictures show cells with and without DNA damage (ssDNA breaks). (**B**) The data show DNA damage measured as percentage of DNA in tail for -/+ fpg treated cells, and are presented as mean ± SEM of three independent experiments. (**C,D**) Cells exposed to different concentrations of EnnB or DMSO for 24 hrs were analyzed for expression of p-p53 (S392) and p21 by Western blotting. Results from one out of two Western blottings are shown. (**E-G**) Cells exposed of EnnB and DMSO for 24 hrs, stained with AF488 coupled AB for p-p53 (SER15) and γH2A.X or stained with FITC coupled AB for p21; and than analyzed by flow cytometry. The presented results comes from one out of two experiments; DMSO (black), EnnB 5 μM (red).

Figure 9. Endocytosis, CTX. RAW 264.7 cells exposed of EnnB 10 μM or DMSO for 24 hrs. (**A**) Shown are pictures of fixed cells incubated with FITC coupled cholera toxin subunit B (Ctx B) (to visualize ganglioside GM1; green and co-stained with DAPI (blue) to detect nuclei (**B**) Pictures of cells incubated with FITCH coupled Ctx B for two hrs before fixation. Original magnification, 200 x.

Figure 10. Characterization by electron microscope. Lysosomal and autophagosomal changes induced by EnnB. Transmission electron microscopic micrographs of RAW 264.7 cells exposed of DMSO (**A**) or EnnB (10 μM; **B**) for 24 hrs. Examples of dysfunctional lysosomes are indicated with white arrows.

Figure 11. Role of caspase 1 activation. RAW 264.7 cells were exposed to EnnB (10 μM; B) 24 hrs while controls were given DMSO only. (**A**) Some of the cells were treated with Caspase1 inhibitor, ZyVAD-FMK (10 μM), 30 min prior to 24 hr exposure with EnnB and DMSO. Cell death were measured by staining the cells with PI/Hoechst and analyzed by use of fluorescence microscope. Presented data is mean ± SEM of three independent experiments. (**B**) Picture and analysis of the protein levels of caspase1 and its cleaved form (p20) in cells exposed of EnnB and DMSO. Samples analyzed by Western blotting. One representative experiment out of three independent experimental setups is shown.

Figure 12. Cytokine release (IL-1β). (**A**)**.** Raw 264.7 cells seeded at 400 000 cells/mL, grown overnight, primed for three hrs with different concentrations of LPS, and exposed for 6 hrs with EnnB (5 μM) or DMSO. Medium analyzed by ELISA. (**B**) Cells seeded at different cell

concentrations, grown overnight, primed for three hrs with LPS (25 ng/mL), and exposed for 6 hrs with EnnB (5 μM) and DMSO. Medium analyzed by ELISA. One representative experiment out of three independent experiments is presented. (**C and D**) Cells seeded at 500 000 cells/mL, grown overnight, primed for three hrs with LPS (25 ng/mL), and exposed for 6 hrs with various concentration of EnnB (2,5, 5 and 10 μM; D) and DMSO. Medium analyzed by ELISA. **(D)** Some cells (+/- LPS) were also treated with ZYVAD-FMK (10 μM), 30 min prior to exposure to EnnB (5 μM) or DMSO. One representative experiment out of three independent experiments is presented, with replicates are shown as means ± SEM.

Figure 13. Role of NF-κB activation. RAW 264.7 cells were exposed to EnnB for 24 hrs while controls were given DMSO only. (**A**) After exposure cells were stained with AF488 coupled AB for NF-κB (p65), and analyzed by flow cytometry. Results from one of two experiments are shown. DMSO (black), EnnB 5 μM (red). The intracellular protein levels of IκBα were measured by Western blotting. (**B**) Shown are results from cells exposed with various concentrations of EnnB (1,25, 2,5 and 5 μM) and DMSO for 24 hrs, experiment done twice. (**C**) Cells primed with LPS for three hrs, followed by 6 hrs exposure with either EnnB (1,25, 2,5 and 5 μM) or DMSO.

FIGURE 1

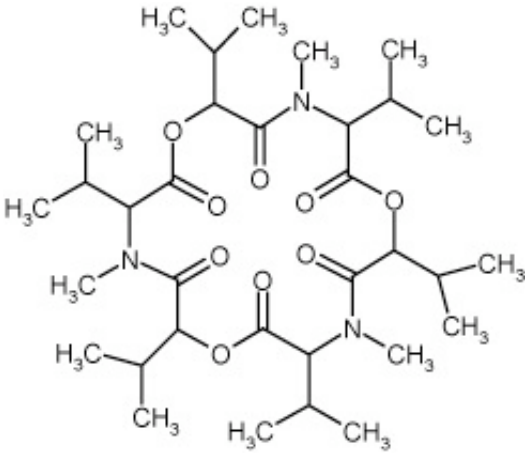
H3C
CH3
CH3
N
CH3
CH3
O
O
O
O
O
CH3
H3C
N
O
O
O
CH3
H3C
CH3
O
N
CH3
CH3
H3C
CH3

FIGURE 2

2A

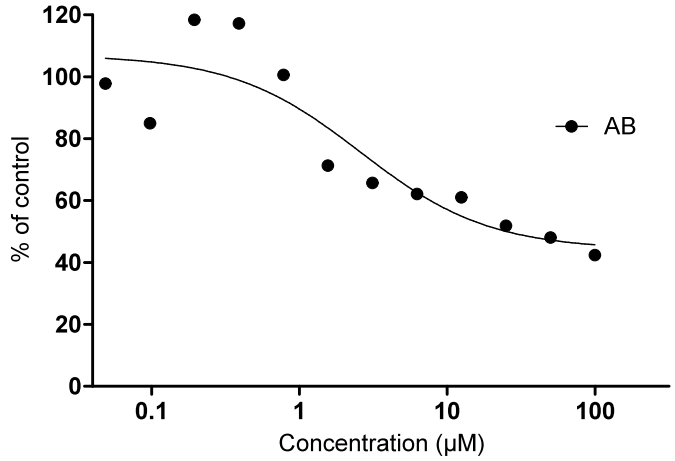

2B

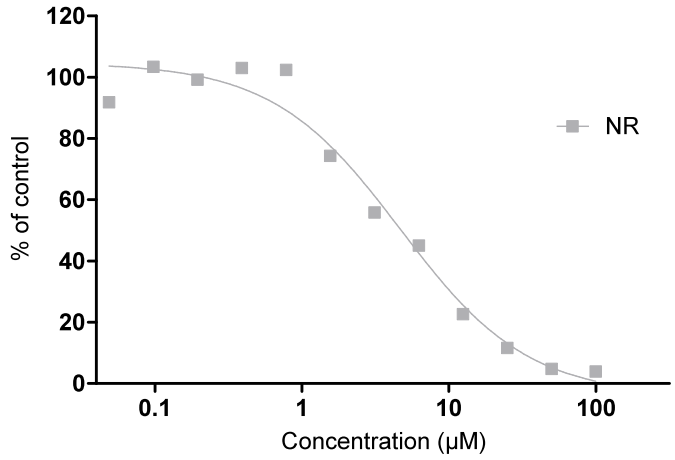

FIGURE 3

3A

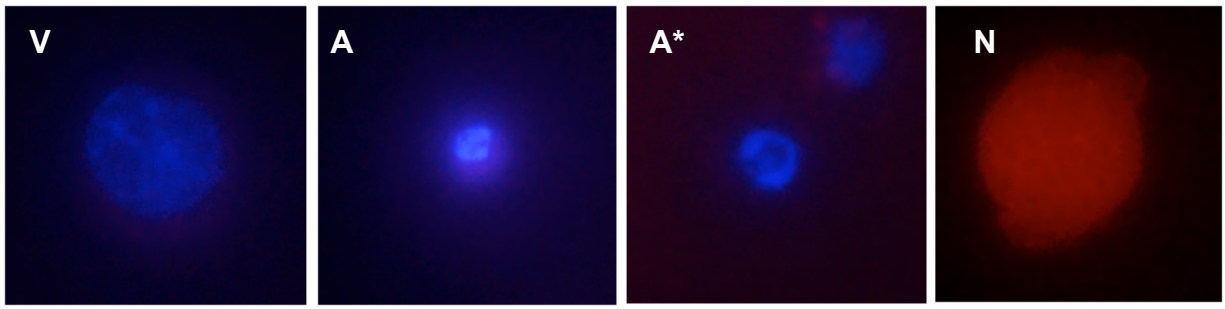

3B

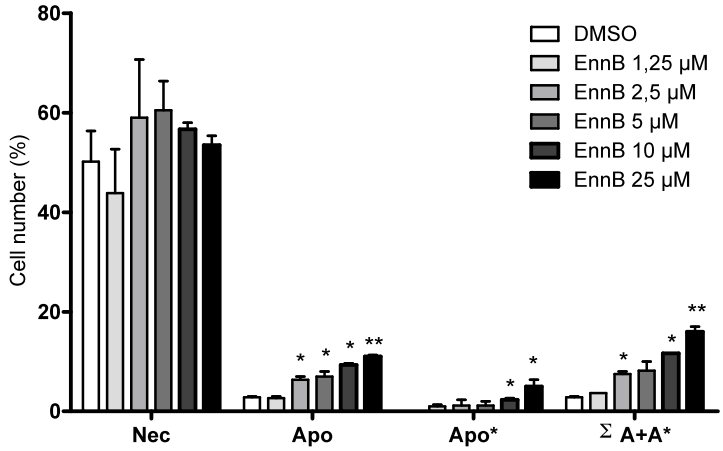

3C

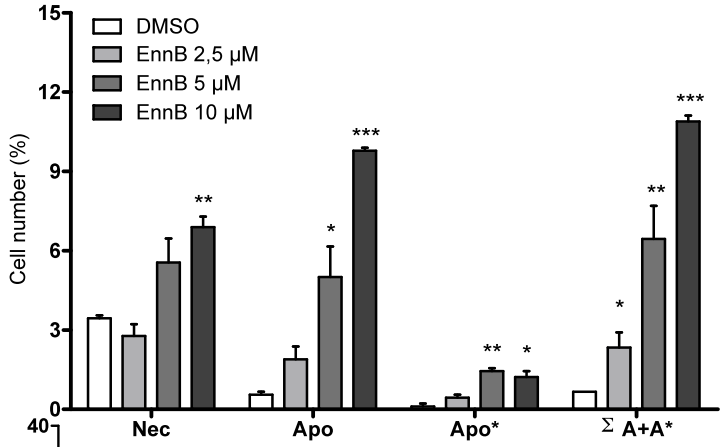

3D

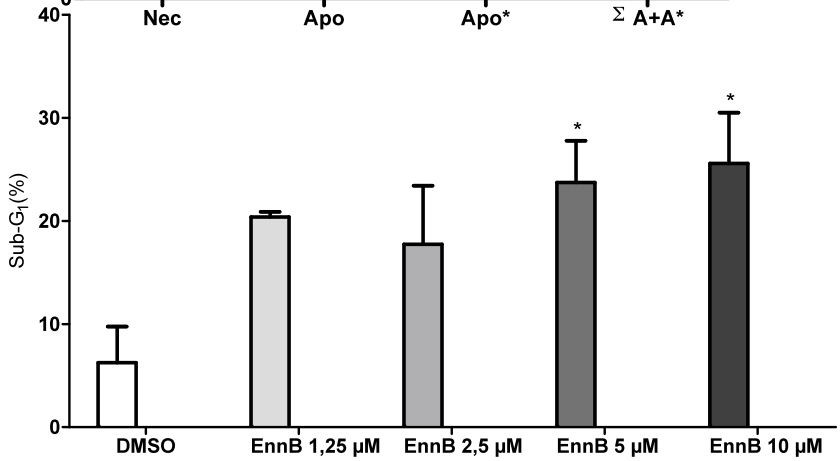

FIGURE 4

4A

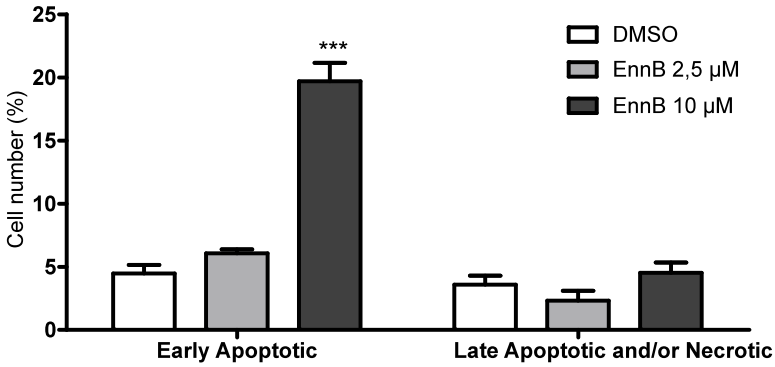

4B

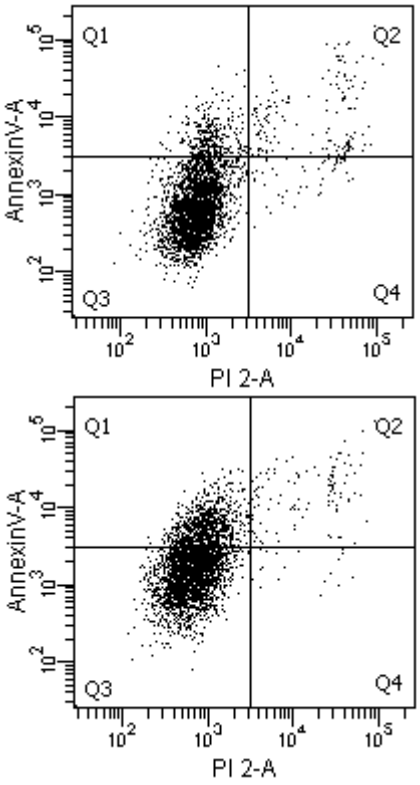

4C

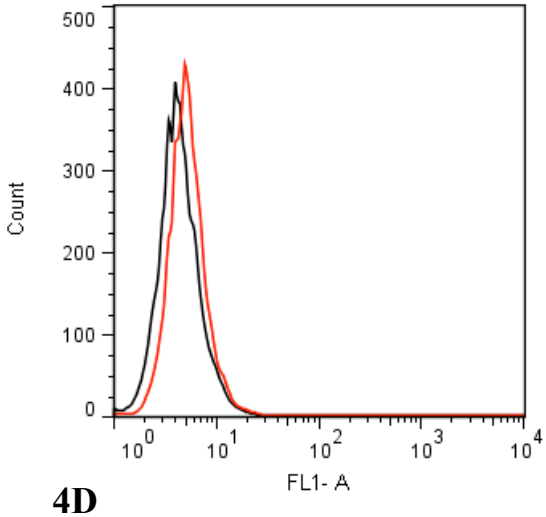

4D

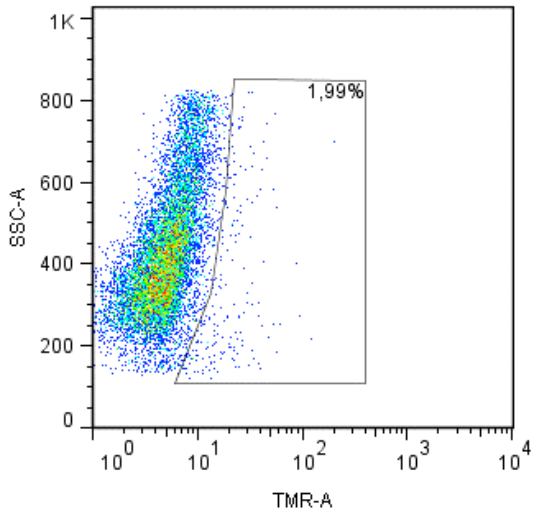

4E

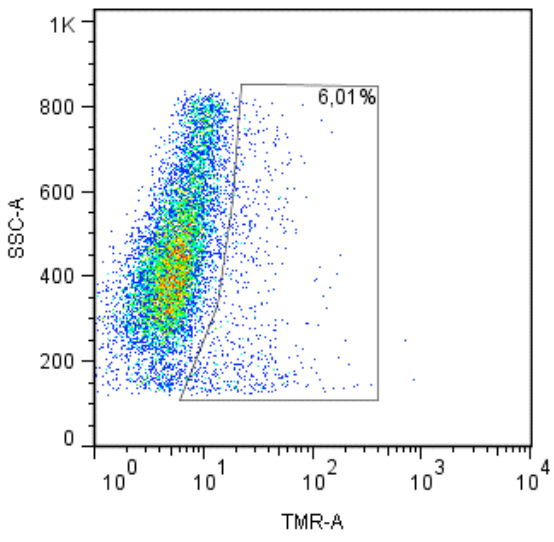

FIGURE 5

5A

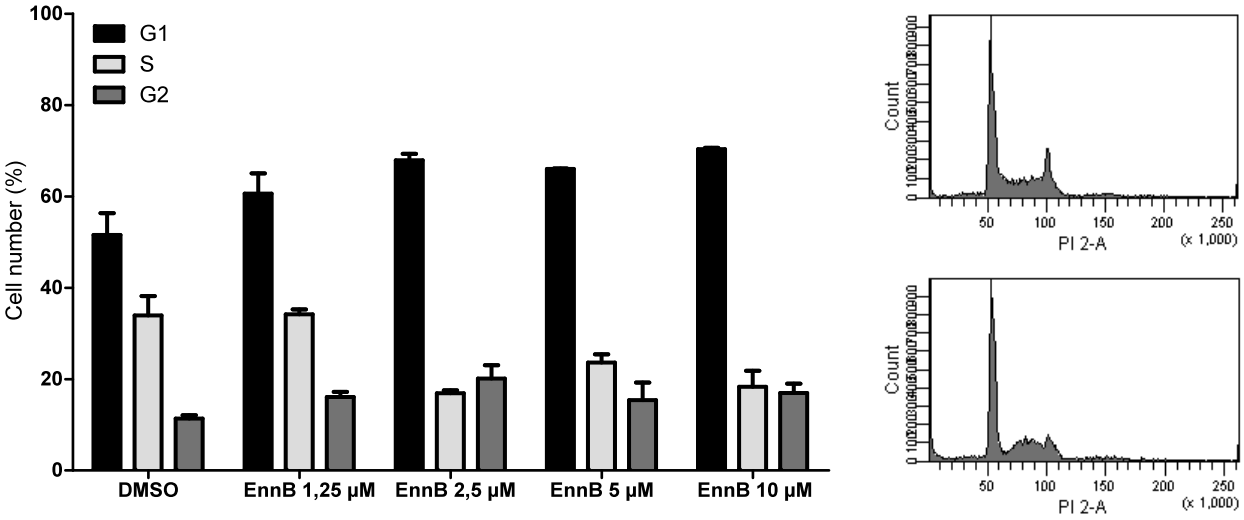

5B

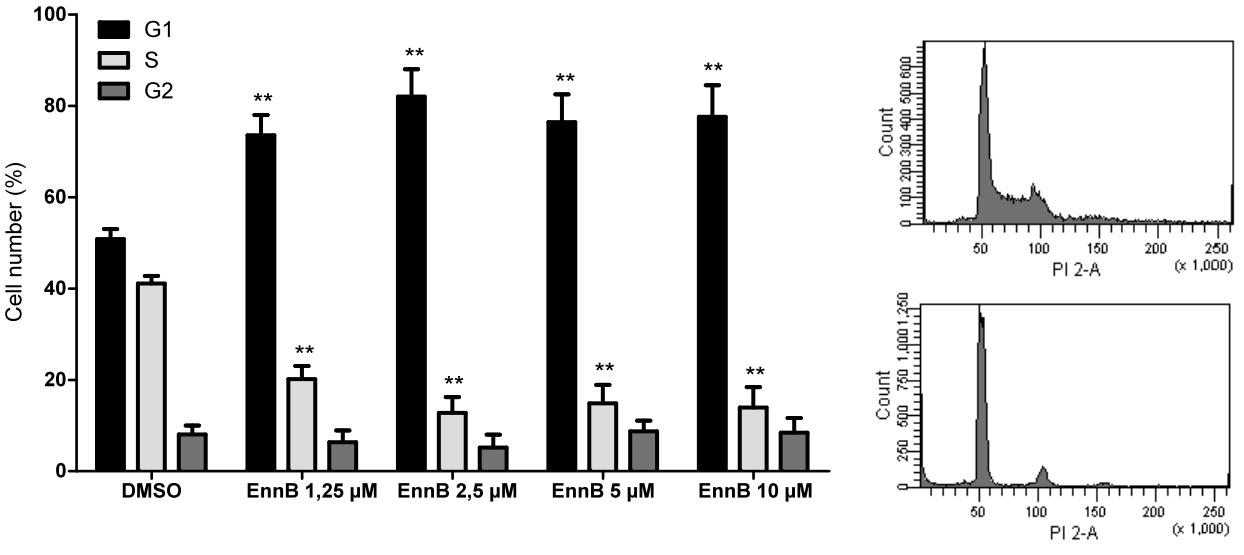

FIGURE 6

6A

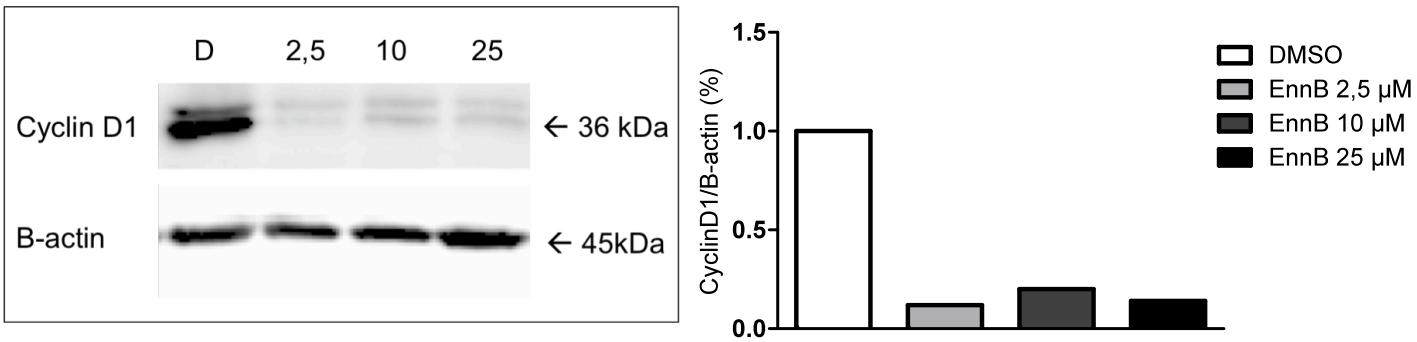

6B

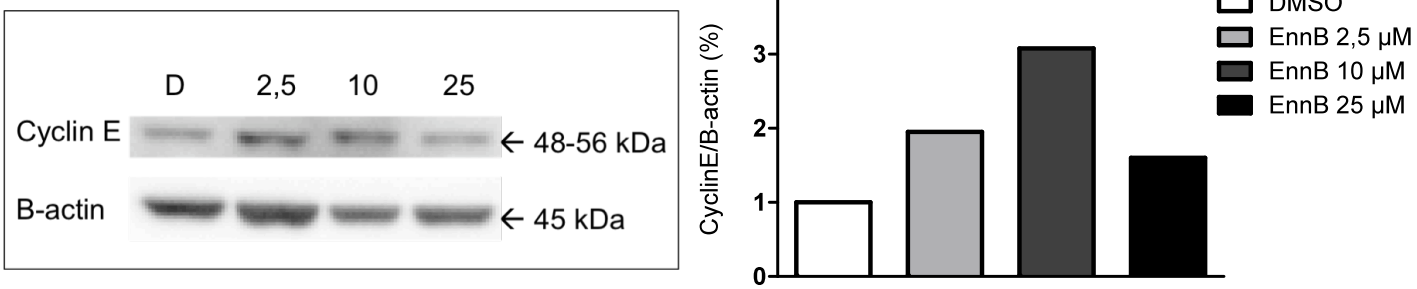

6C

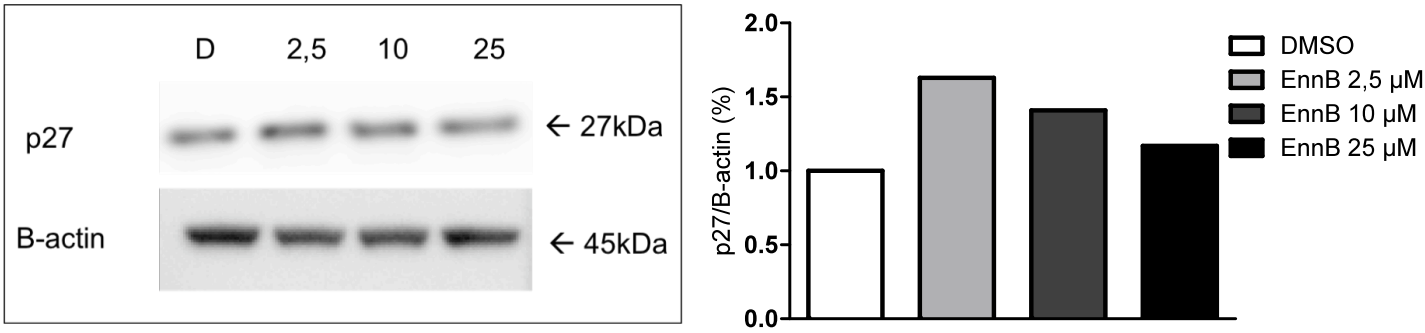

FIGURE 7

7A

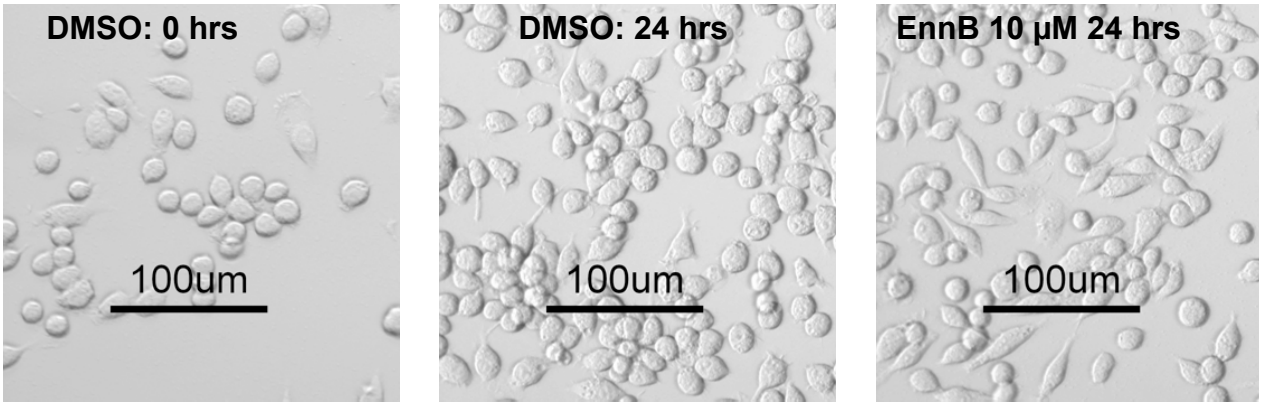

7B

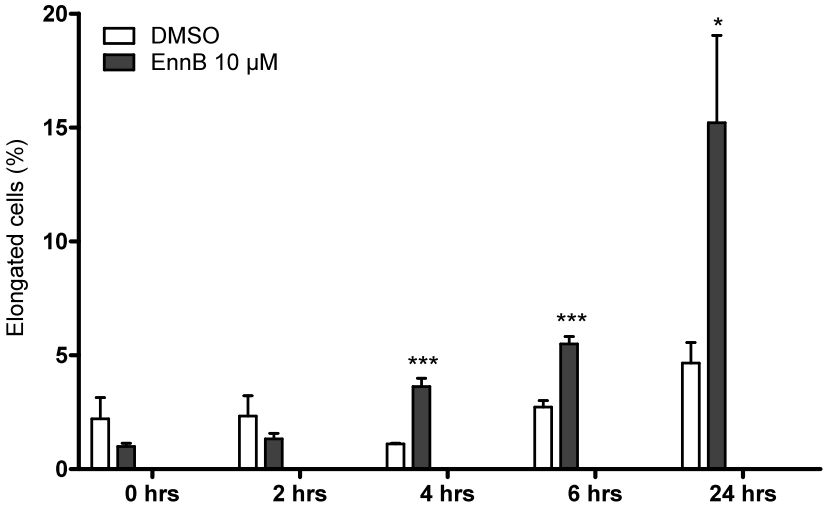

7C

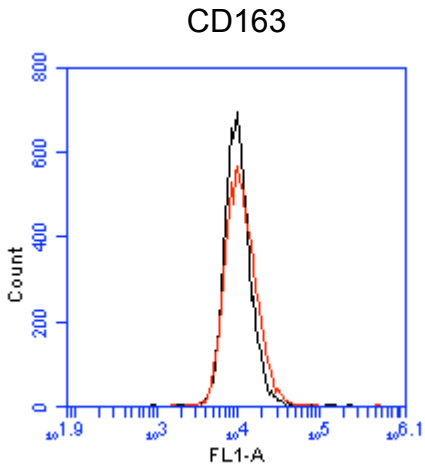

7D

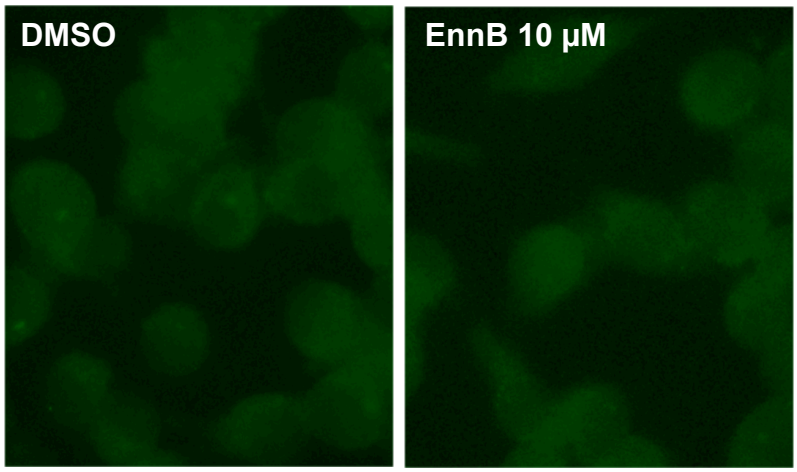

FIGURE 8

8A

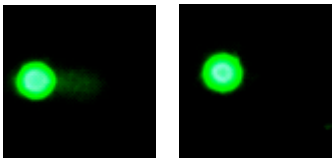

8B

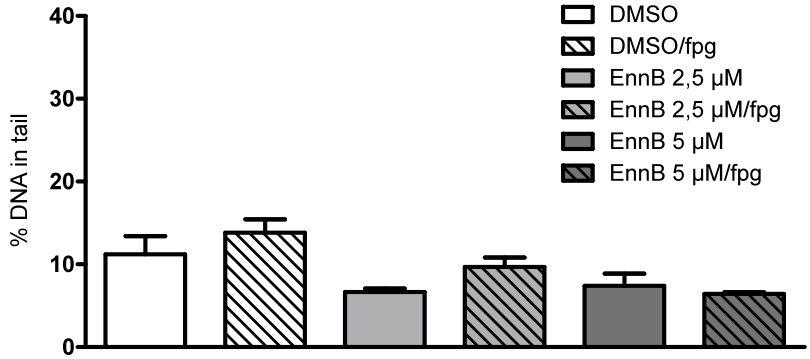

8C

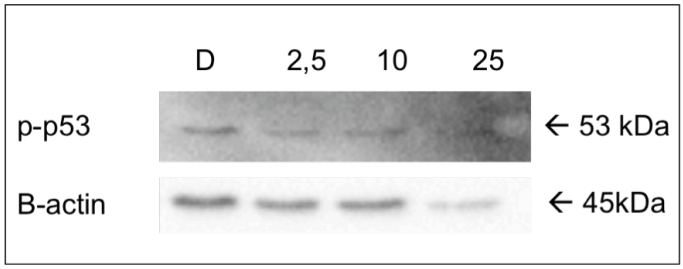

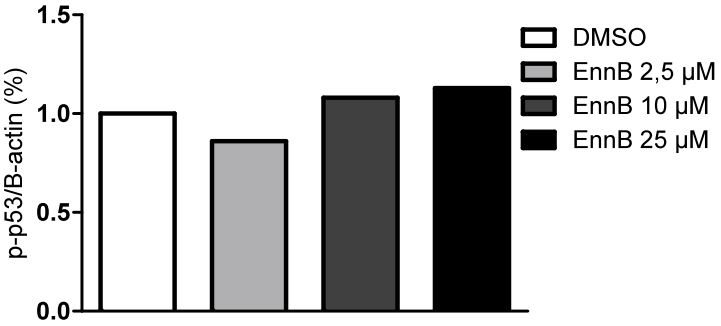

8D

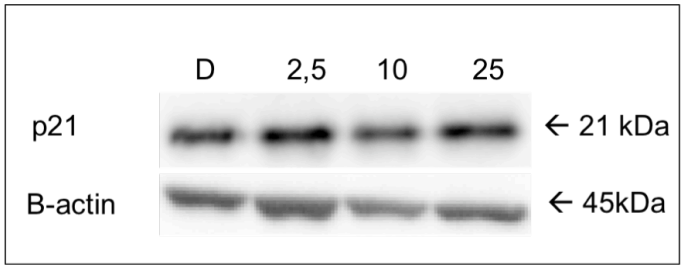

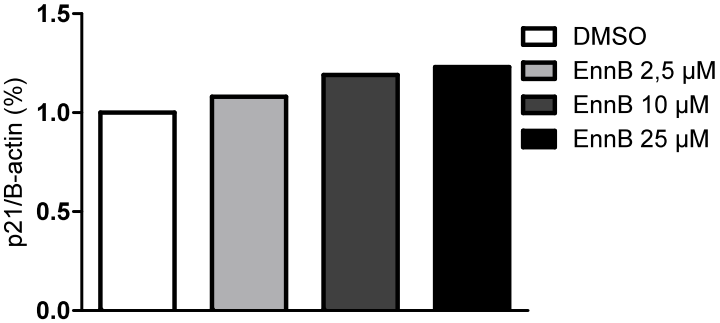

8E

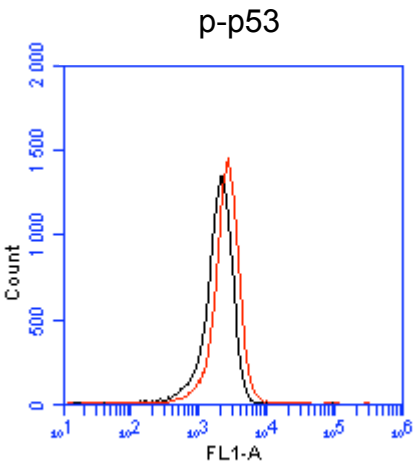
p-p53
Count
2 000
1 500
1 000
500
0
FL1-A

8F

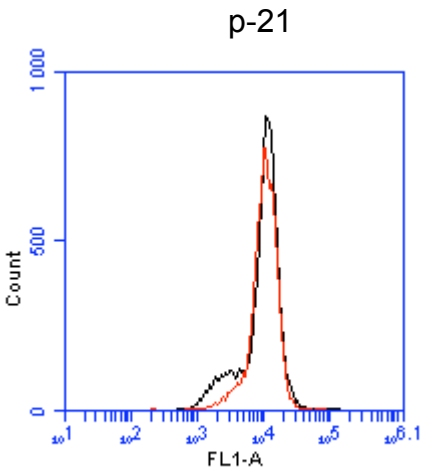
p-21
Count
1 000
500
0
FL1-A

8G

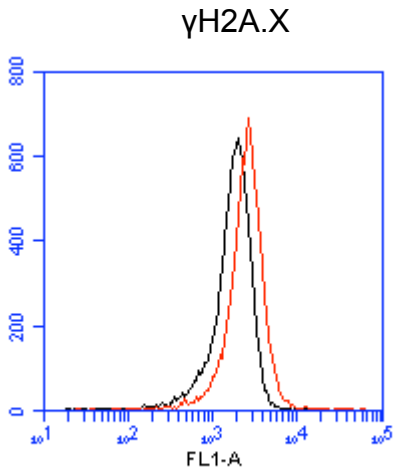
γH2A.X
800
600
400
200
0
FL1-A

FIGURE 9

9A

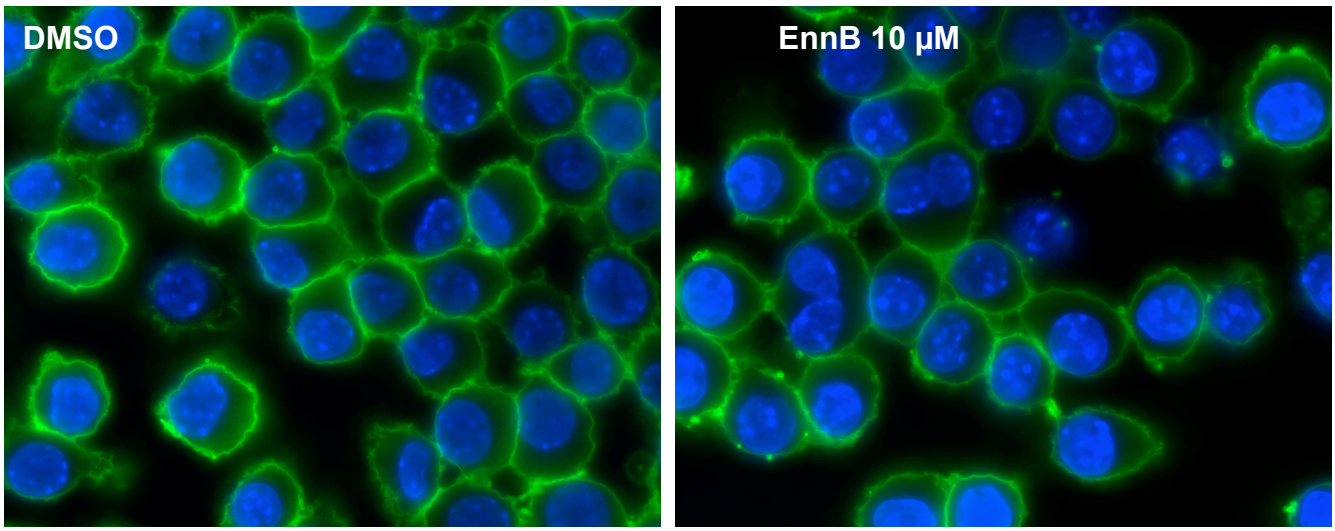

9B

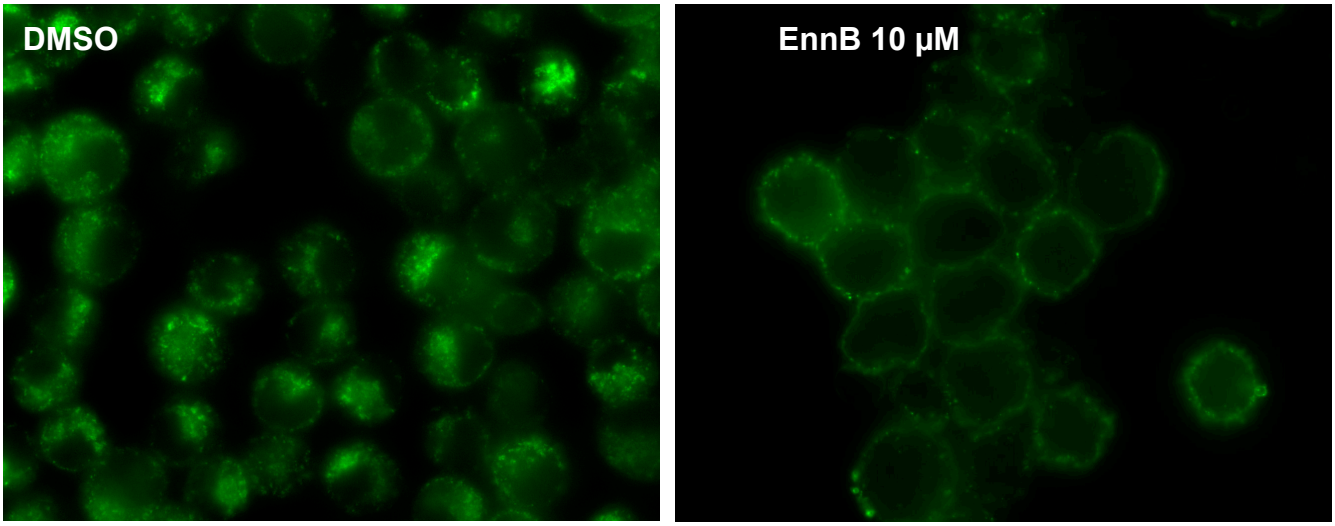

FIGURE 10

10A **10B**

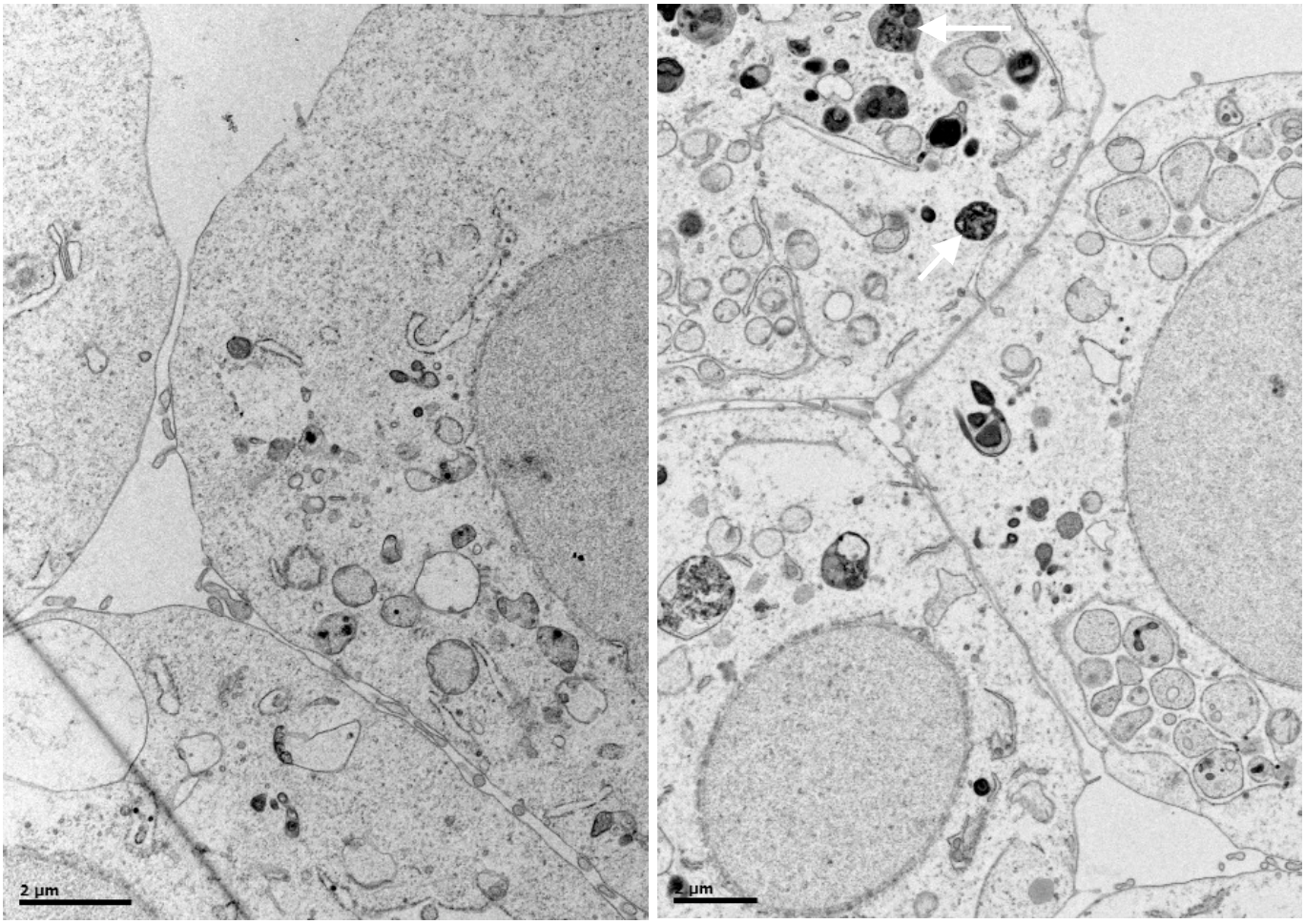

FIGURE 11

11A

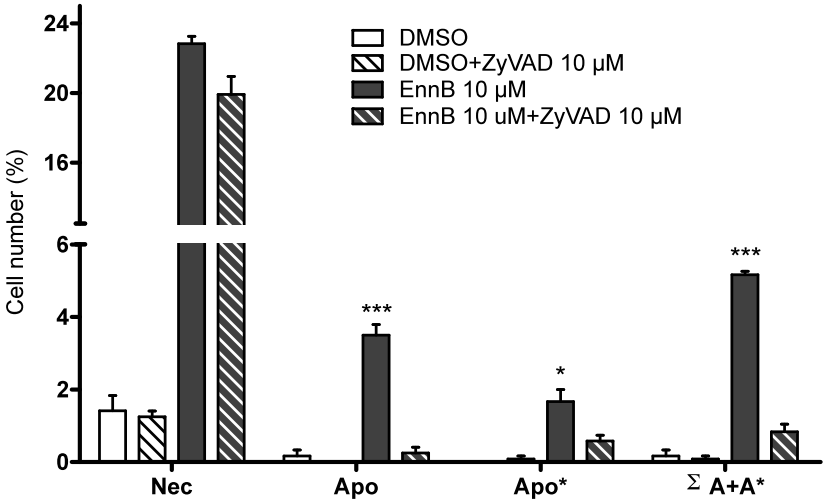

11B

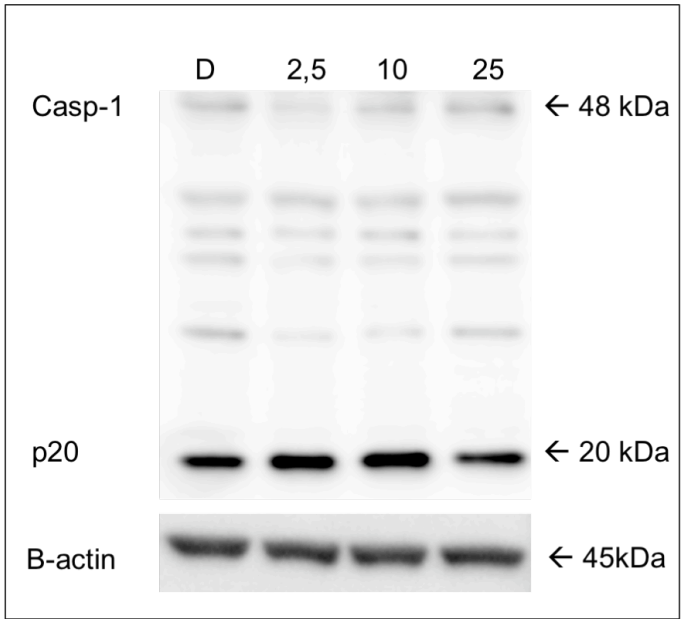

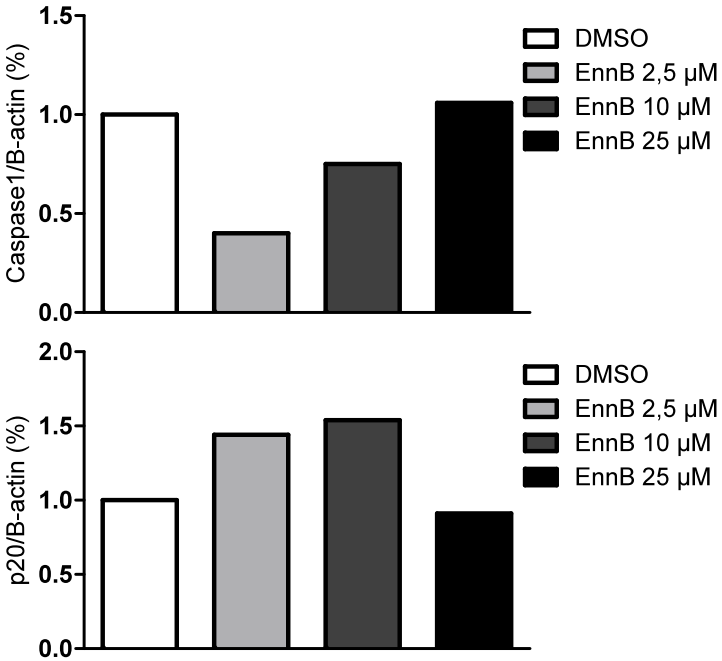

FIGURE 12

12A

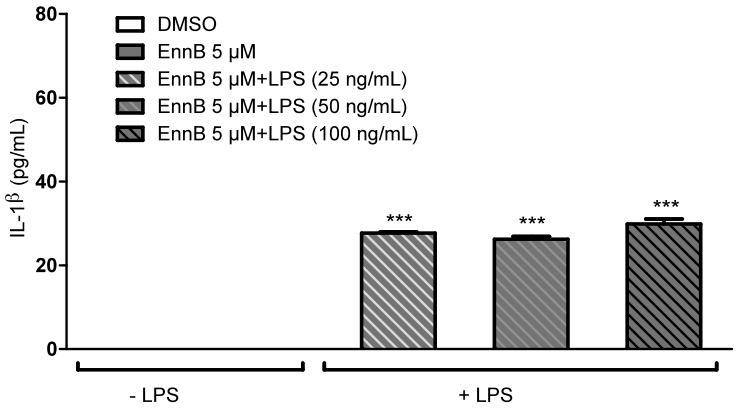

12B

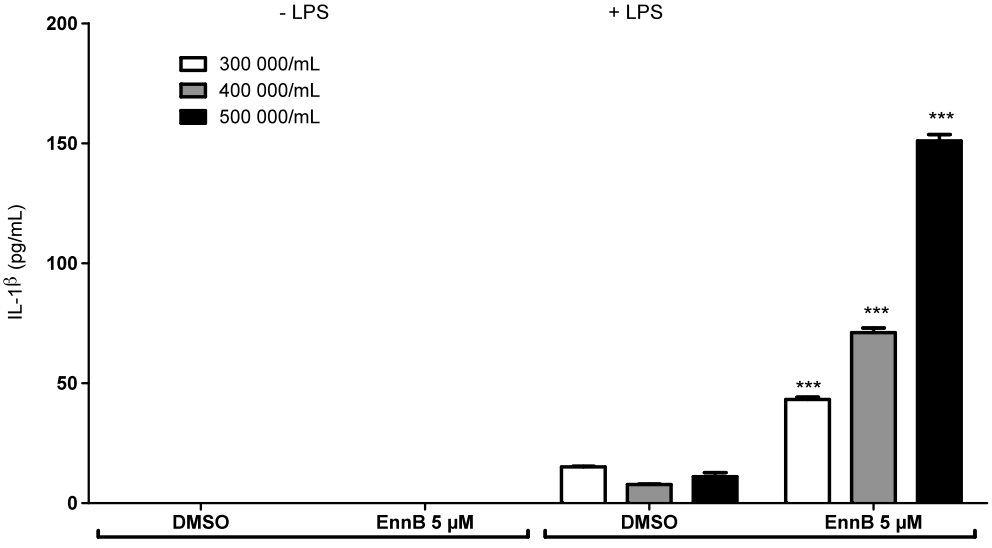

12C

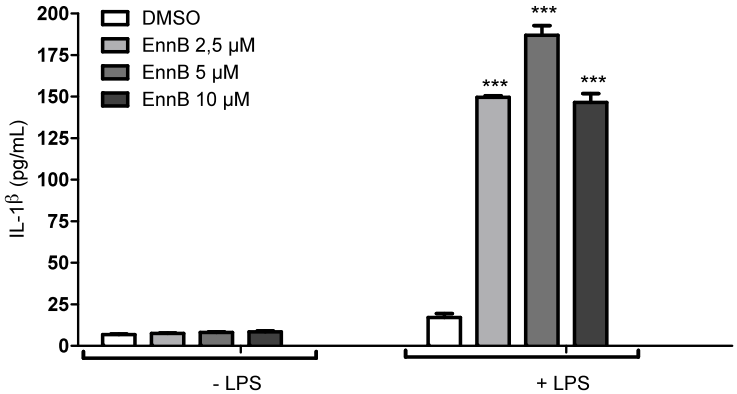

12D

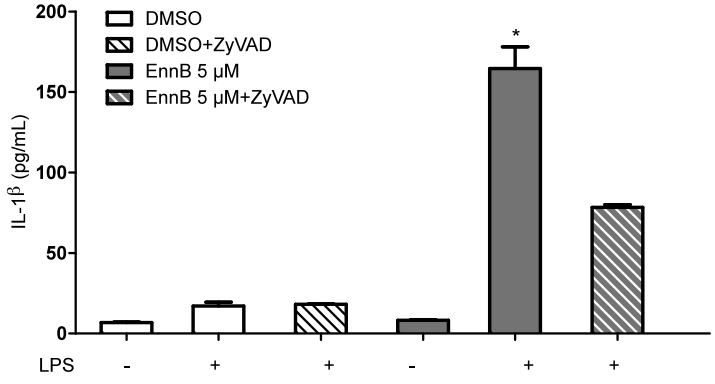

FIGURE 13

13A

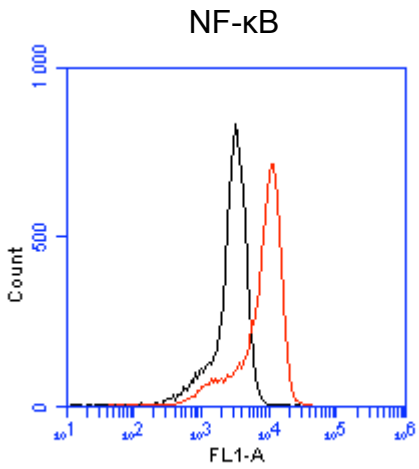

13B

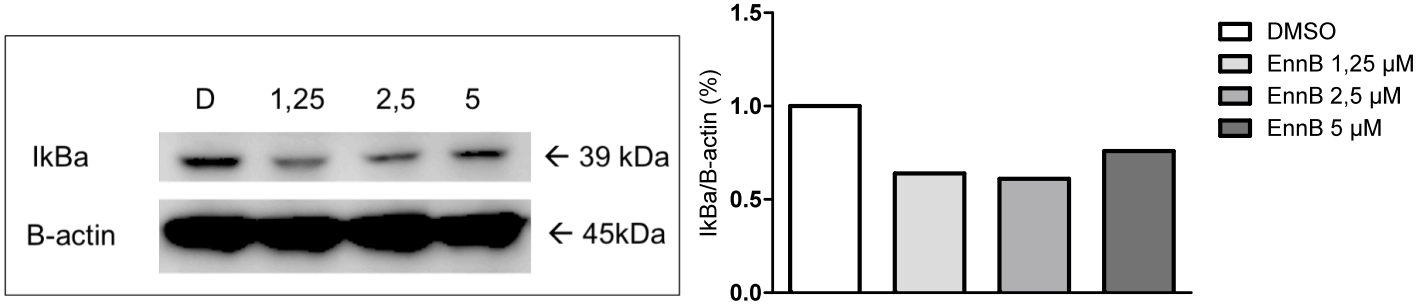

13C

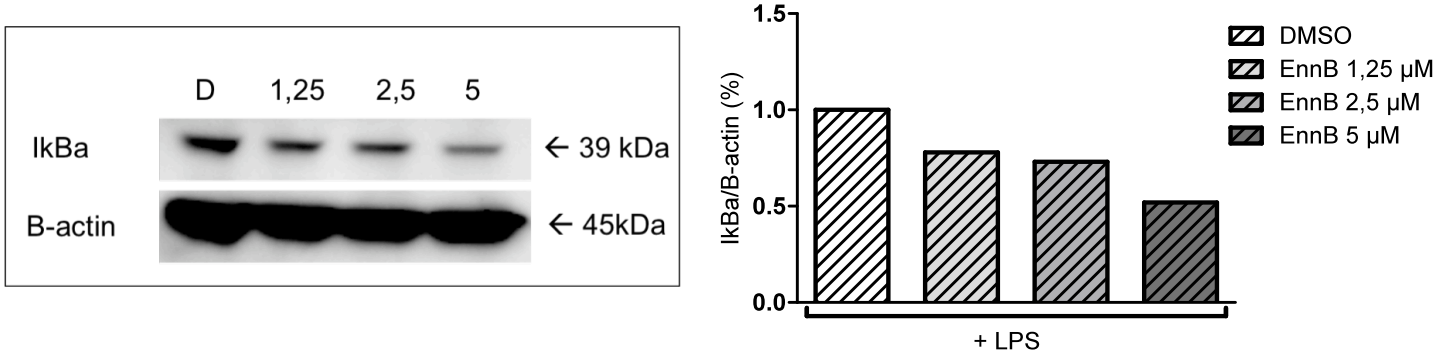

Figure legends, supplementary results

Figure I. Cell cycle analysis. J774A.1 cells cultured in UpCell dishes and exposed with different concentrations of EnnB (1,25, 5, 10 μM) or DMSO for 24 hrs. All cells were stained with PI and analyzed with flow cytometer. Presented data is mean ± SEM of three independent experiments.

Figure II and III. Changes in morphology. (**VI**) J774A.1 cells grown in UpCell™ dishes, exposed of EnnB (5 μM) and DMSO for 24 hrs, stained with AF488 coupled AB for CD163, and analyzed by flow cytometry; DMSO (black), EnnB (red). The results from one out of two experiments are presented (**VII**) Cells exposed of EnnB (10 μM) and DMSO for 6 hrs, and stained with AF488 coupled AB for CD163. Original magnification, 100 x.

Figure IV, V, VI and VII. Cytokine release (IL-1β). (**IV**)**.** J774a.a cells seeded at 400 000 cells/mL, grown overnight, primed for three hrs with different concentrations of LPS, and exposed for 6 hrs with EnnB or DMSO. Media analyzed by ELISA. (**V**) Cells seeded at different cell concentrations, grown overnight, primed for three hrs with LPS (25 ng/mL), and exposed for 6 hrs with EnnB and DMSO. Medium analyzed by ELISA. One representative experiment out of three independent experiments is presented. (**VI**) Cells seeded at 600 000 cells/mL, grown overnight, primed for three hrs with LPS (25 ng/mL), and exposed for 6 hrs with EnnB and DMSO. Medium analyzed by ELISA. (**VII**) Some cells (+/- LPS) were also treated with ZyVAD-FMK (10 μM), 30 min prior to exposure to EnnB (5 μM) or DMSO. One representative experiment out of three independent experiments is presented and the replicates are shown as means ± SEM.

I

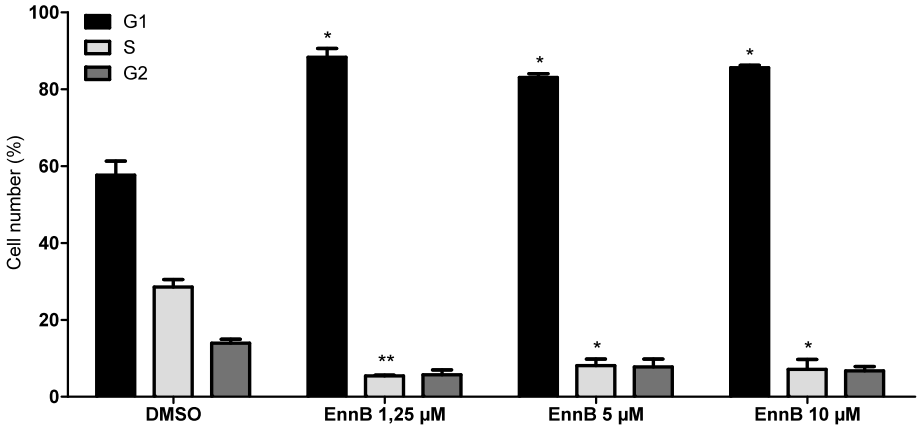
100
80
60
40
20
0
Cell number (%)
G1
S
G2
*
**
*
*
*
*
DMSO
EnnB 1,25 µM
EnnB 5 µM
EnnB 10 µM

II

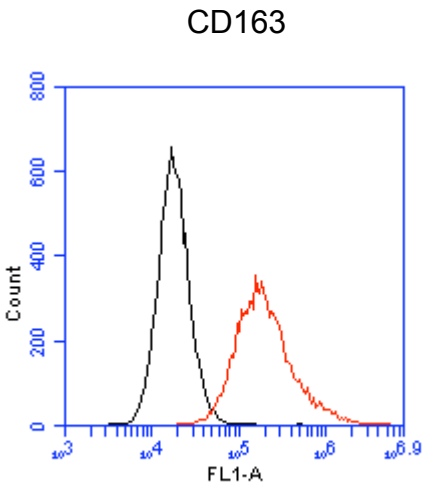
CD163
800
600
400
200
0
Count
10^3
10^4
10^5
10^6
$10^{6.9}$
FL1-A

III

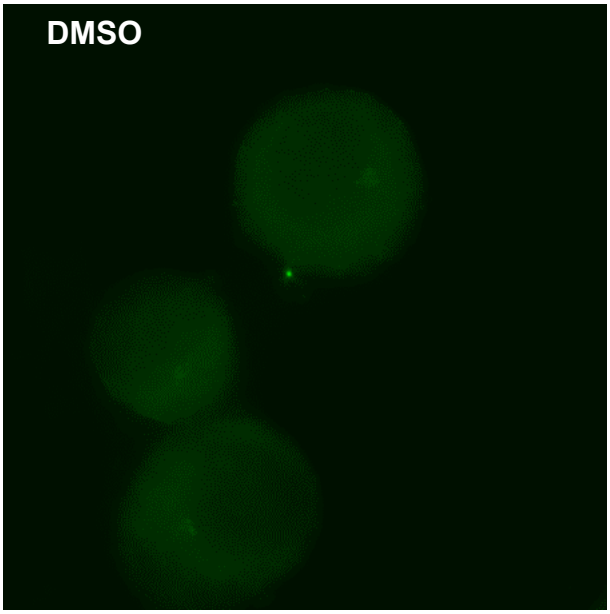
DMSO

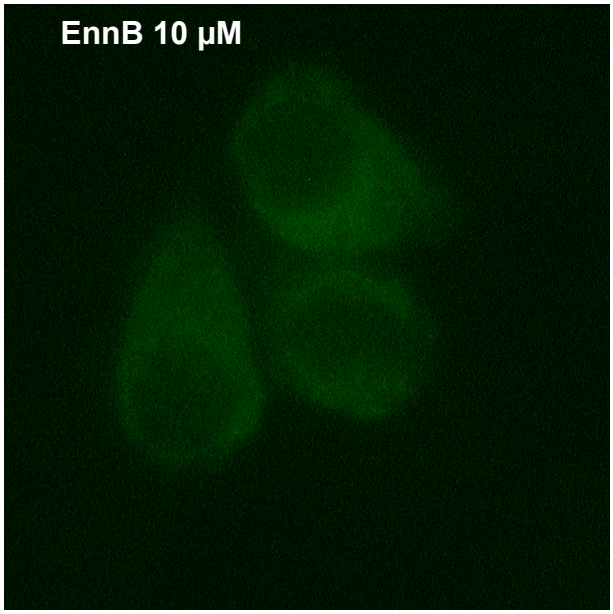
EnnB 10 μM

IV

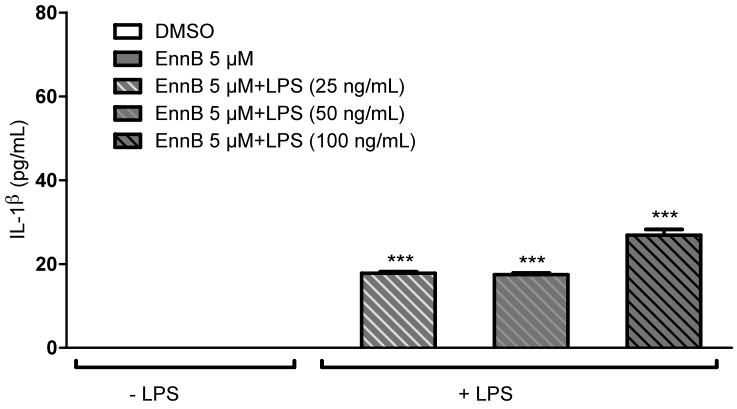
DMSO
EnnB 5 µM
EnnB 5 µM+LPS (25 ng/mL)
EnnB 5 µM+LPS (50 ng/mL)
EnnB 5 µM+LPS (100 ng/mL)
IL-1β (pg/mL)
0
20
40
60
80
***
***
***
- LPS
+ LPS

V

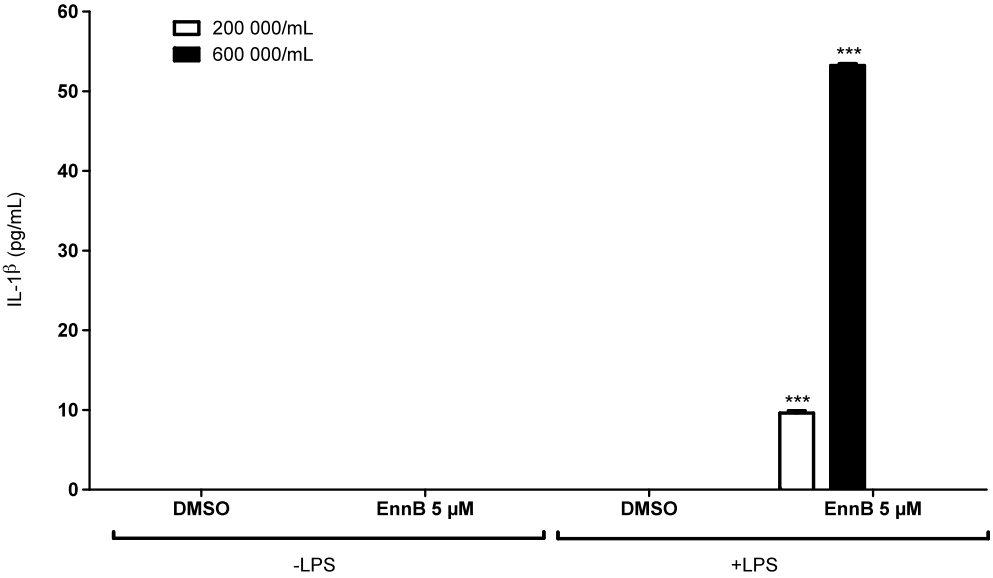
200 000/mL
600 000/mL
IL-1β (pg/mL)
0
10
20
30
40
50
60
***
***
DMSO
EnnB 5 µM
DMSO
EnnB 5 µM
-LPS
+LPS

VI

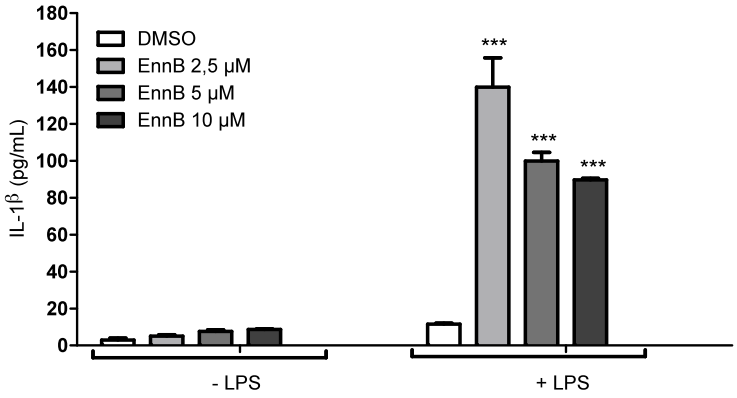
DMSO
EnnB 2,5 µM
EnnB 5 µM
EnnB 10 µM
IL-1β (pg/mL)
0
20
40
60
80
100
120
140
160
180
***
***
***
- LPS
+ LPS

VII

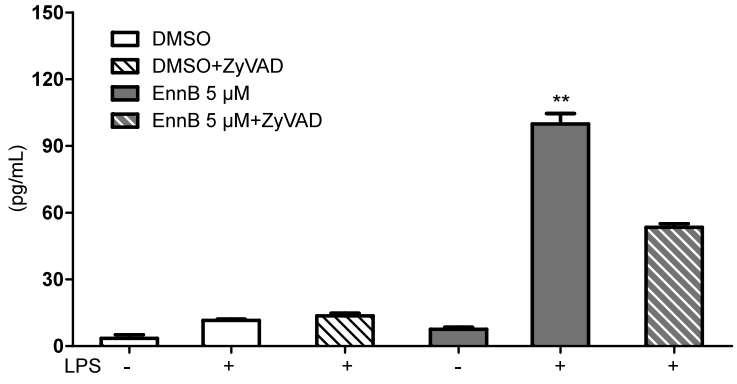
DMSO
DMSO+ZyVAD
EnnB 5 µM
EnnB 5 µM+ZyVAD
(pg/mL)
0
30
60
90
120
150
**
LPS - + + - + +